Elsevier Editorial System(tm) for Journal of Catalysis

Manuscript Draft

Manuscript Number: JCAT-16-151R1

Title: On the stability and nature of adsorbed pentene in Brønsted acid zeolite H-ZSM-5 at 323 K

Article Type: Research paper

Keywords: molecular dynamics
zeolites
catalysis
Density functional theory
adsorption

Corresponding Author: Prof. Veronique Van Speybroeck,

Corresponding Author's Institution: Ghent University

First Author: Julianna Hajek

Order of Authors: Julianna Hajek; Jeroen Van der Mynsbrugge; Kristof De Wispelaere; Pieter Cnudde; Louis Vanduyfhuys, Doctor; Michel Waroquier; Veronique Van Speybroeck

UNIVERSITEIT GENT

FACULTY OF **ENGINEERING AND ARCHITECTURE**

Center for Molecular Modeling

Joachim Sauer
Editor Journal of Catalysis

Dear Editor,
Dear Joachim,

Herewith we have the pleasure to resubmit the paper entitled : **"On the stability and nature of adsorbed pentene in Brønsted acid zeolite H-ZSM-5 at 323 K" by J. Hajek , J. Van der Mynsbrugge, K. De Wispelaere , P. Cnudde, L. Vanduyfhuys, M. Waroquier and V. Van Speybroeck,** for publication in Journal of Catalysis.

We have received the comments of two reviewers which were very positive and which suggest publication subject to some major/minor revisions. We have taken them all into account in the revised version. In separate documents we give a substantial reply to the reviewers that carefully addresses the issues raised in the reviewer's comments.
We have added an author (Louis Vanduyfhuys) in the list. During the revision process he has given a very constructive contribution in a correct thermodynamic analysis of the metadynamics results. As requested by one of the reviewers, we re-analyzed all our MD results. We hope that you are willing to accept this slight change in the author list.

We further hope that the manuscript is now suitable for publication.

Sincerely,

Prof. dr. ir. V. Van Speybroeck
Center for Molecular Modeling – Ghent University
Technologiepark 903,
9052 Zwijnaarde
E-mail: veronique.vanspeybroeck@ugent.be

***Revision Notes**

Reply to reviewer #1 :

We thank the reviewer for his/her careful reading of the manuscript with manuscript number JCAT-16-151. We try to give a valuable reply to all comments which were all very constructive. Reviewer's comments are printed in blue.

1. The DFT calculations have been carried out at 0 K by optimizing the geometry at the RPBE+D3 level and then conducting single point calculations with other functionals. While the general conclusions drawn from the calculations are independent of the functional chosen, it would be very useful to know whether geometry optimization with a better functional would change the conclusion about the relative stability of the π-complex and alkoxide structures.

The authors completely agree with the major concern of the reviewer regarding the reliability of the geometry optimization based on one level of theory (PBE+D3). This functional has proven to be reliable in many periodic static calculations on nanoporous materials, but to remove any doubt we performed new geometry optimizations and frequency calculations for 2-pentene π- complex and 2-pentoxide using BEEF-vdW functional . [1] Geometrical details of the selected structures with PBE-D3 and BEEF-vdW functionals are given in Table 1. The comparison of free energy ΔG and enthalpy ΔH differences between BEEF-vdW //PBE D3 and BEEF-vdW // BEEF-vdW is given in Table 2.

Table 1: Geometrical details of the selected structures with PBE-D3 and BEEF-vdW functionals

2-pentene π-complex				
	C2-H	C3-H	C1C2C3C4	C2C3C4C5
PBE-D3	2.015	2.049	-174.5	-135.3
BEEF-vdW	2.146	2.214	-175.3	-135.1
2-pentoxide				
	C – O		C1C2C3C4	C2C3C4C5
PBE-D3	1.558		-62.9	-172.1
BEEF-vdW	1.577		-63.3	-171.2

Table 2: Free energy ΔG and enthalpy ΔH differences for configurations for the π-complex and chemisorbed complex in H-ZSM-5 at 323 K given in kJ/mol.

	BEEF-vdW //PBE D3		BEEF-vdW // BEEF-vdW	
	ΔG	**ΔH**	**ΔG**	**ΔH**
2-pentene (π) -> 2-pentoxide	53.27	41.96	51.05	42.7

The energy differences are very similar with each other, and support the conclusions made in the paper. These additional results have been included in Table 2 of the main manuscript.

2. At the top of page 10, the authors state that static calculations systematically overestimate the enthalpy of adsorption of the π-complex because optimized geometries are used, which bring the alkene closer to the BAS. Since different levels of theory are used for the static and dynamic, it would be interesting to know the extent to which this matters. It would also be important to show that the dynamic calculations are intrinsically more correct with respect to experimental measurements for, say butene or propene.

We thank the reviewer for this remark and reformulated the sentence slightly. The origin of larger adsorption enthalpies for the π-complex is indeed related to usage of optimized geometries, which take into account only one point on the potential energy surface. Our MD simulations show that in reality at finite temperatures, the π-complex can adopt various geometries leading to a probability distribution as shown in Figure 3 of the main manuscript. This distribution in terms of the C-Hz distance is asymmetric, which results on average in free energies of adsorption which are higher in MD simulations than in static calculations. We expect that with lower temperatures the width of the probability curves would become narrower around the maximum at 1.9 Å, and that in the limit T $\rightarrow$ 0 K also MD will predict a distance between alkene and BAS that coincides with the static value. We believe that this conclusion is not dramatically affected by the slightly different levels of theory used in the static and dynamic calculations (PBE + D3 versus revPBE + D3). Our reply on issue #1 shows that adopting another level of theory does not lead to crucial differences on the optimized geometries.

3. While the results of the metadynamics calculations are consistent with those obtained from the MD calculations, here again it is important to establish whether the level of theory used for the two types of calculations is important or not.

This is a more complex issue as ab initio MD and MTD simulations are very expensive even with revPBE+D3 as functional. Use of more contemporary functionals in MD simulations is practically excluded and not yet done in literature. We agree that such an attempt will be very instructive, but currently not feasible, despite the very powerful computer facilities about which we dispose

Since this manuscript is limited to examining alternative modes of computing the enthalpy and Gibbs free energy of pentene adsorption, the authors need to make sure that the conclusions drawn are not an artefact of the computational methods drawn.

We refer to the additional static calculations with BEEF + vdW where we clearly demonstrate that different computational methods don't affect the conclusions. Alternative enhanced MD methods to compute enthalpy and Gibbs free energies exist (e.g. umbrella sampling) and we are trying to apply them to the reaction transforming the π-complex to the alkoxide, but such an investigation is not realizable within a period of 5 weeks (the period for submission of a revised version of the manuscript). But we fully agree that such a study would be very instructive to sustain the reliability of methods such like metadynamics.

1. Wellendorff, J., et al., *Density functionals for surface science: Exchange-correlation model development with Bayesian error estimation.* Physical Review B, 2012. **85**(23): p. 235149.

Reply to reviewer #2 :

We thank the reviewer for his/her careful reading of the manuscript with manuscript number JCAT-16-151. We try to give a valuable reply to all comments which were all very constructive. Reviewer's comments are printed in blue.

1.) The finite-temperature calculations were performed for T=323K but the authors did not explain why they selected this particular value. This information should be added.

This is a very good question, as the adsorption behavior of alkenes largely depends on the temperature. There is no specific reason why we took T = 323 K as finite temperature for the molecular dynamics and metadynamics calculations. This temperature has been inspired by our former collaboration with Prof.J.Lercher of the Department of Chemistry and Catalysis Research Center in Munchen, who did adsorption experiments and reactions of linear pentene on Brønsted acid zeolites at T = 323 K. Inspection of the different adsorption studies in the literature learns that linear alkenes have barely been investigated experimentally in contrast to alkanes due to the high reactivity of alkenes. Although experimental conditions may not be extracted from alkane adsorption studies to alkene, they give an indication about the relevant temperature range, the more that the amount of experimental information on alkane adsorption is much more available. Most of the measurements have been performed in a temperature range around room temperature. [1] If we limit the literature survey to the most recent publications, we refer to a recent combined experimental-theoretical paper [2] where experimental isotherms of ethane and propane on chabazite have been measured at 313 K. Also pure theoretical studies investigated the adsorption properties of alkanes around 300 K. The effect of temperature on the adsorption of short alkanes in SSZ-13 has been investigated by Jiang et al. [3] at temperatures of 250, 275, 325 and 350 K. Goltl and Hafner [4] calculated adsorption energies for alkanes at 300 K.

Experimental measurements on linear-alkene adsorption in zeolites are not available. An old measurement dates from 1982 reporting a physisorption enthalpy of 1-butene in MFI at 300 K. The same temperature is considered by Gomes et al. [5] in an extended QM/MM procedure to calculate adsorption enthalpies of light hydrocarbons in both acidic and neutral zeolite MFI. There exist some scarce studies on branched butenes and pentenes. These experiments have been taken place at temperatures around 298 K. Isobutene conversion on H-ZSM-5 with formation of *tert*-butyl cation has been experimentally investigated in the temperature range 298 to 473 K. [6] The formation of *tert*-butyl cation upon protonation of isobutene by Brønsted acid sites has also been studied theoretically by Tuma and Sauer [7] and at temperatures higher than 120 K the *tert*-butyl cation has been found to be more favored over the alkoxides, and this behavior did not change in the examined temperature range 200 – 400 K.
We agree that we focus our work at one specific temperature, and that we may not extrapolate the theoretical results obtained at 323 K to other temperatures as the reactivity of alkenes is heavily sensitive to temperature. Investigation of the temperature dependence on the adsorption properties of alkenes in zeolites is highly interesting and instructive. We are currently working on this item, but this is not really the focus of the current manuscript. Moreover an extensive number of additional MD runs are necessary to fully answer the question about temperature dependence of the results. This is beyond the scope of the current manuscript. We added a sentence in the

manuscript which indicates that 323 K is a representative temperature to study the adsorption behavior at low temperatures.

2.) p. 5, line 5: the name of Hirshfeld is misspelled ("Hirschfeld" -> "Hirshfeld")

It is a typo, and we corrected it.

3.) p. 5, l. 3-5 in the second paragraph: "…was successfully used in earlier zeolite catalysis work.[59-61]". The indicated references 59-61 have nothing to do with earlier catalysis work as the sentence seems to suggest. Please provide the correct reference.

Indeed, it is not the intention to cite the work of Parrinello here. Instead we meant the following references:
J.Van der Mynsbrugge et al. [8]
S.Moors et al. [9]
K.De Wispelaere et al. [10]

4.) the choice of collective variables used in metadynamics and their exact definition is an essential piece of information that should be presented in the main text and not in supplemental material (Fig. S2)

We have transferred the technical details of the MTD to the Supporting Information to save space in the main manuscript. We agree that the choice of the collective variables (CVs) is an essential part of any MTD run and therefore we added the definition of the two selected CVs in the main manuscript as requested by the reviewer.

5.) If I have understood correctly, the static calculations are performed to investigate the effect of various vdW corrections on adsorption energetics (and the MD calculations with most of these methods would be too time-consuming). I find the way the authors chose to discuss these results a bit unfortunate. The problem is that the presentation of the static adsorption enthalpies follows immediately after the presentation of the MD results on distribution of various geometric parameters and the reader is left to wonder why the heats of adsorption were not computed directly from MD (as is indeed done two pages later). I suggest to discuss the static calculations after complete presentation of all MD results (including energetics). The motivation for performing static calculations should be clearly stated and the numerical results should be presented in the main text, not in SI.

For the same reason as in comment #4 we inserted the table with “static” energetics originally in the SI as it takes a full page. However, we agree that the table contains a lot of computational data which are not trivial to obtain in the periodic VASP calculations and which deserve more attention than in the previous manuscript. Therefore we followed the reviewer and added this table to the main manuscript. In addition as requested by the second reviewer, we performed additional static calculations with another functional (BEEF + vdW) [11] to investigate the influence of the level of theory on the obtained geometries and energies. Previously, all the energetic calculations (free energy ΔG and enthalpy ΔH differences) using different levels of theory were based on the same

geometry of the π-complex and chemisorbed complex obtained in PBE-D3. We also added these new calculations to the main manuscript (Table 2).

The reviewer also suggests to discuss the static calculations after complete presentation of all MD results including the energetics. We understand the viewpoint of the reviewer, however we opted to maintain the current ordering of results based on following rationale. We first want to discuss the MD simulations to explore the flat potential energy surface and to determine the most frequently visited structures. These may serve than as input for the static calculations. By first performing an MD run, we are reassured that we have selected appropriate structures for the static calculations. Our static calculations show that some finite temperature features may not be captured by the 0 K approach, which give a motivation to further present more extensive MD results.

6.) p. 9, l.6 , second paragraph: the term "free enthalpy" is mentioned by "enthalpy" is meant (the former term is sometimes used as synonym for the Gibbs free-energy), please correct

We corrected it in the manuscript.

7.) p. 9, the result: "The adsorption enthalpies of pentoxides obtained as an ensemble average in the MD simulations are closer to the values obtained with static approaches." is in contrast to expectation as the alkoxy species are more tightly bound to the framework than the physisorbed species and hence the geometry and energetics of MD-generated configurations should be much closer to those for potential energy minimum. The authors should provide a reasonable explanation for the quoted statement.

MD-generated configurations predict a spreading of the distance between the pentoxide and the frame (C-O_z) which is less marked than in case of the π-complex. The probability distribution in Figure 2 shows a relatively narrow peak around 1.5 – 1.6 Å. Static calculations predict similar distances for the pentoxides, but shorter values for the π-complexes. If the distance between the adsorbed species and the frame is some measure for the adsorption enthalpy we may assume some equal values for the pentoxide formation in both static and dynamic approaches. In the same spirit we expect a higher adsorption enthalpy for the pentene π-complex in the static approach. Within this context the enthalpies of adsorption of the pentoxides, as resulting from the MD simulations, are closer to the static predictions. These observations also confirm that the covalent bond between the framework and the hydrocarbon remains in place throughout the simulation. The alkoxy species are indeed more tightly bound to the framework than the π-complexes, but this does not necessarily leads to a larger adsorption enthalpy. Specific non-bonded interactions between the π-electrons of the double bond and the Brønsted acid site make π-complexes more bound than the physisorbed states, which undergo only a weak van der Waals interaction with the walls of the zeolite. The difference in stabilization energy has not been computed, but is estimated to be in the range of 26 - 32 kJ/mol based on the heat of adsorption of n-pentane in H-ZSM-5 (-62 kJ/mol) [1] . This partly explains the apparent contradiction as quoted in the comment of the reviewer.

8.) in my experience, the setting used in the metadynamics calculations (high frequency of Gaussian addition (0.04 fs-1) + large height of Gaussians (1 kJ/mol)) is not sufficient to achieve a reasonable accuracy for computed free-energies (this is evident also from the shape of free-energy profiles (Fig.

5)) and hence the analysis of free-energetics should be considered as qualitative only. This should be clearly indicated in the manuscript. If the authors are convinced that they achieved accuracy allowing them to make even quantitative analysis (Tab. 1) they should explain why they think so.

Computed free energies predicted by metadynamics are indeed mainly qualitative, as they largely depend on the choice of the collective variables and other degrees of freedom. In addition, the shapes of the free- energy profiles displayed in Figure 5 are not helping us to extract accurate energetics. But they give an indication of the free-energy barriers and reaction free energies. We added in the manuscript some sentences making it more clearly.

We also started MTD simulations with a lower frequency in adding smaller Gaussian hills but the calculations demand an extremely high computational cost, and unfortunately are not terminated in the course of the five weeks to finalize the revised manuscript. To be more concrete: in the new simulations the height of the initial hills were set to 2 kJ/mol instead of 5 kJ/mol, and the frequency was reduced by a factor of two (100 time steps instead of 50) . A rough estimate of the required computer time comes to 50 days without any delay. If we add some extra days for analyses, we need at least two months to achieve this computational task.

9.) there is a serious problem with expression used to compute free-energy of activation (p. 4. In SI) - clearly, the term in logarithm corresponds to probability density and is therefore, in general, not dimensionless (indeed, it has unit of 1/(product of units of CVs used in simulation)) as it should be (otherwise the units of free-energy would be wrong). This formula must be corrected such that the expression is invariant with respect to the change of units of CV and all numerical results must be updated accordingly.

We thank the reviewer for this important remark. We agree there is a dimensionality conflict with the given expression of the free-energy of activation, which can be traced back to fundamental thermodynamic principles. This issue requests a lot of attention and is not trivial. We start with a brief summary of elementary concepts of statistical physics to make our point clear and transparent. The free energy of a system in thermodynamic equilibrium is related to its partition function (in the classical limit):

$$G = -k_B T \ln Z$$

$$Z = \frac{1}{h^{3N} N!} \int d\boldsymbol{x}^N d\boldsymbol{p}^N e^{-\beta H(\boldsymbol{x}^N, \boldsymbol{p}^N)}$$

Suppose we are interested in the probability distribution as function of a collective variable *s*, which may be a bond length, an angle, a coordination number,… At first instance we rewrite the partition function as:

$$Z_q(s) = \frac{1}{h^{3N} N!} \int d\boldsymbol{x}^N d\boldsymbol{p}^N \, \delta(Q(\boldsymbol{x}^N, \boldsymbol{p}^N) - s) e^{-\beta H(\boldsymbol{x}^N, \boldsymbol{p}^N)}$$

$$Z = \int_{-\infty}^{+\infty} Z_q(s) ds$$

with $Z_q(s)ds$ the contribution to the partition function due to a microstate with a value of s in the range [s,*s+ds*]. Furthermore, one can rewrite the equation above in terms of a probability distribution $P_q(s)$:

$$P_q(s) = \frac{Z_q(s)}{Z}, \qquad \int_{-\infty}^{+\infty} P_q(s)ds = 1$$

However, if we would define the free energy of such a microstate as:

$$G_q(s) = -k_B T \ln Z_q(s)$$

we immediately notice a problem, because $Z_q(s)$ has the dimension of $[s]^{-1}$. One possible way to resolve this issue is by considering differences in free energies at two different values of *s*:

$$G_q(s_2) - G_q(s_1) = -k_B T \ln \frac{Z_q(s_2)}{Z_q(s_1)} = -k_B T \ln \frac{P_q(s_2)}{P_q(s_1)} \quad \left(= -k_B T \ln \frac{Z_q(s_2)ds}{Z_q(s_1)ds}\right)$$

The ratio of the probability distributions in the argument of the logarithm defines whether it is more probable to find the system in the range [s_2,s_2+*ds*] than to find it in the range [s_1,s_1+*ds*], or vice versa. The ratio $\frac{P_q(s_2)}{P_q(s_1)}$ also defines whether $G_q(s_2) > G_q(s_1)$ or $G_q(s_2) < G_q(s_1)$. This is also exactly how this free energy difference should be interpreted.

Alternatively, one could define a **macrostate** A for which s lies in the range [s_1,s_2]. This gives rise to the following expressions:

$$\begin{aligned}
Z_A &= \int_{s_1}^{s_2} Z_q(s)ds \\
P_A &= \frac{Z_A}{Z} \\
G_A &= -k_B T \ln Z_A = -k_B T \ln \frac{Z_A}{Z} - k_B T \ln Z \\
G_A &= -k_B T \ln P_A + G
\end{aligned}$$

In this case Z_A, must be interpreted as the contribution to the partition function from the macrostate A. Similarly G_A can be interpreted as the free energy associated with the macrostate A which can be computed up to a constant G, which is the total free energy. Finally, if we can assume that the partition function has a constant value of $Z_q(\bar{s})$ in that range [s_1,s_2], the equations reduce to:

$$\begin{aligned}
Z_A &= Z_q(\bar{s})\Delta s \\
P_A &= \frac{Z_q(\bar{s})\Delta s}{Z} \\
G_A &= -k_B T \ln Z_q(\bar{s})\Delta s
\end{aligned}$$

with $\bar{s} = \frac{s_1+s_2}{2}$ and $\Delta s = s_2 - s_1$.

Given this background, we may explain the problem raised by the reviewer. We computed a free energy profile $G_q(s)$, which we now want to use to estimate the difference in free energy between two states: state **R** representative for the reactants, and state **TS** representative for the transition states. The choice of these states can be done according to the two approaches outlined above. In

the first approach, we identify **R** with the microstate corresponding to the minimum of $G_q(s)$ in the reactant valley and **TS** with the microstate corresponding to the maximum of $G_q(s)$. This gives rise to:

$$\Delta G^{\ddagger} = G_q(s_{TS}) - G_q(s_R)$$

This method entails just taking the free energy difference between the maximum of the free energy profile and the minimum, which is the most crude approximation.

The second approach consists in dividing the complete range for s into three regions **R**=]-∞,s_0], **TS** =[s_0, s_1] and **P** = [s_1, +∞[, or more if the trajectory encounters more than 1 TS. Now we can compute:

$$Z_R = \int_{-\infty}^{s_0} Z_q(s)\,\Delta s \frac{ds}{\Delta s} = \int_{-\infty}^{s_0} e^{-\beta G_q(s)}\,\Delta s \frac{ds}{\Delta s} \;;\; G_R = -k_B T \ln Z_R = -k_B T \ln \int_{-\infty}^{s_0} e^{-\beta G_q(s)}\,\Delta s \frac{ds}{\Delta s}$$

$$Z_{TS} = \int_{s_0}^{s_1} Z_q(s)\,\Delta s \frac{ds}{\Delta s} = \int_{s_0}^{s_1} e^{-\beta G_q(s)}\,\Delta s \frac{ds}{\Delta s} \;;\; G_{TS} = -k_B T \ln Z_{TS} = -k_B T \ln \int_{s_0}^{s1} e^{-\beta G_q(s)}\,\Delta s \frac{ds}{\Delta s}$$

$$Z_P = \int_{s_1}^{+\infty} Z_q(s)\,\Delta s \frac{ds}{\Delta s} = \int_{s_1}^{+\infty} e^{-\beta G_q(s)}\,\Delta s \frac{ds}{\Delta s} \;;\; G_P = -k_B T \ln Z_P = -k_B T \ln \int_{s_1}^{+\infty} e^{-\beta G_q(s)}\,\Delta s \frac{ds}{\Delta s}$$

To circumvent the dimensionality conflict here, we introduced Δs and defined $Z_q(s)\,\Delta s = e^{-\beta G_q(s)}$, which is inspired by the equation $G_A = -k_B T \ln Z_q(\bar{s})\,\Delta s$.

Having introduced free energies to regions , we are now able to define free energies of activation $\Delta G^{\ddagger}$ as :

$$\Delta G^{\ddagger} = G_{TS} - G_R = -k_B T \ln \frac{\int_{s_0}^{s_1} e^{-\beta G_q(s)} ds}{\int_{-\infty}^{s_0} e^{-\beta G_q(s)} ds},$$

and reaction free energies ΔG_r :

$$\Delta G_r = G_P - G_R = -k_B T \ln \frac{\int_{s_1}^{+\infty} e^{-\beta G_q(s)} ds}{\int_{-\infty}^{s_0} e^{-\beta G_q(s)} ds}$$

Δs drops out of the equation, so it does not influence the results.

As the referee pointed out, the expression presented in the manuscript was confusing and would only be correct in the limit that the region [s_0, s_1] corresponds to one bin.

We now reanalyzed our MTD data using both approaches sketched above. Both methods above do not suffer from a dimension issue. The first approach does not account for the width of the valley., whereas the second method does. Since the width of a certain valley can have large entropic contributions that we wish to take into account, we choose to use the second approach.

For the three reactions under study we define five regions : the reactants R (in this region local minima and hills are present), the transition state TS1 with the formation of the pentyl intermediate, the intermediate area I, the transition state TS2 to form the alkoxide and finally the product region P. The different areas are easily recognized in the figures which are attached.

The width of the TS region (s_0, s_1) is determined by the thermal fluctuation, which is given by the standard deviation of the collective variable s. We have systematically taken a value of 0.04,

which represents the average of the thermal fluctuations measured at the local minima of the reactant valley. This is a highly reliable value, and for the six transition states in the three reactions it corresponds with 2 – 5 bins.

In the tables we report the free energies of activation and the reaction free energies resulting from the method outlined above. We also include the gap between maximum and minimum of the free energy profile which represents a crude approximation of the barrier. Similarly, for the reaction free energies we also report the differences between the lowest state of the reactant region and the product region.

complete trajectory	**barrier**		
	original paper	method 2	TS - Gmin
1-pentene->2-pentyl	33	36.8	34.9
2-pentyl-> 2 pentoxide	20	20.3	16.4
2-pentene-> 2-pentyl	42	38.2	37.9
2-pentyl-> 2-pentoxide	17	12.1	11.8
2-pentene-> 3-pentyl	92	84.7	88.8
3-pentyl-> 3-pentoxide	48	54.6	55.1

complete trajectory via basin between the TS's	**reaction free energy**		
	original paper	method 2	crude
1-pentene->2-pentyl	+9	-2.3	-0.9
2-pentyl -> 2-pentoxide	-14	-9.2	-14.6
2-pentene-> 2-pentyl	+5	+2.8	+3.1
2-pentyl -> 2-pentoxide	-19	-15.2	-17.0
2-pentene -> 3-pentyl	+24	+22.9	+24.9
3-pentyl -> 3-pentoxide	+27	+34.3	+35.3

complete trajectory	**reaction free energy**		
	original paper	method 2	crude

1-pentene->2-pentoxide	-5	-11.5	-15.4
2-pentene-> 2-pentoxide	-14	-12.4	-13.9
2-pentene -> 3-pentoxide	+51	+57.2	+60.2

In the revised manuscript we take up the results obtained by the second method . They don't affect the discussion on the MTD results made in the original manuscript. In the SI we give a short outline of the applied methodology .

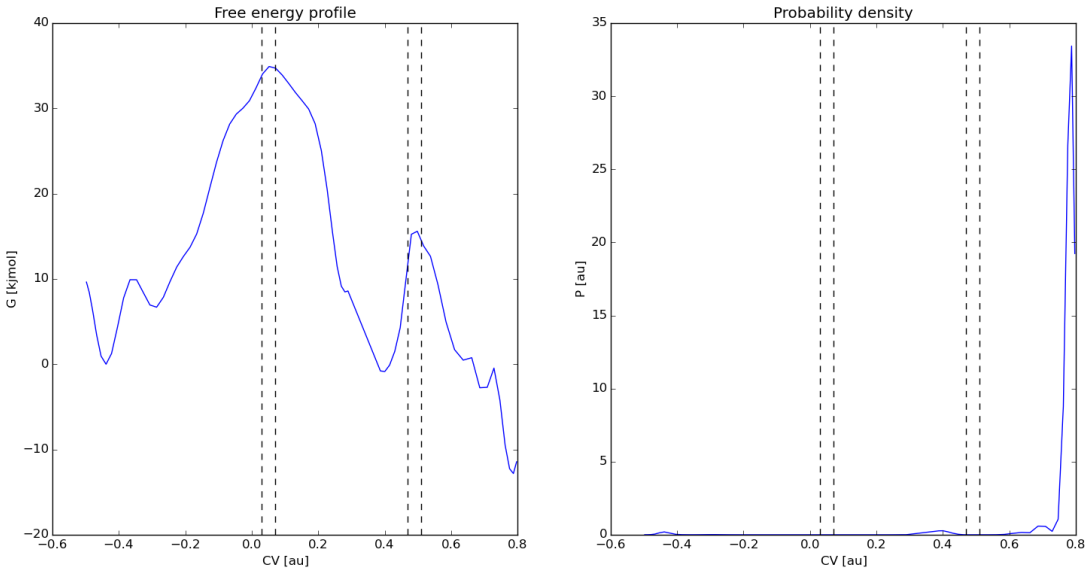

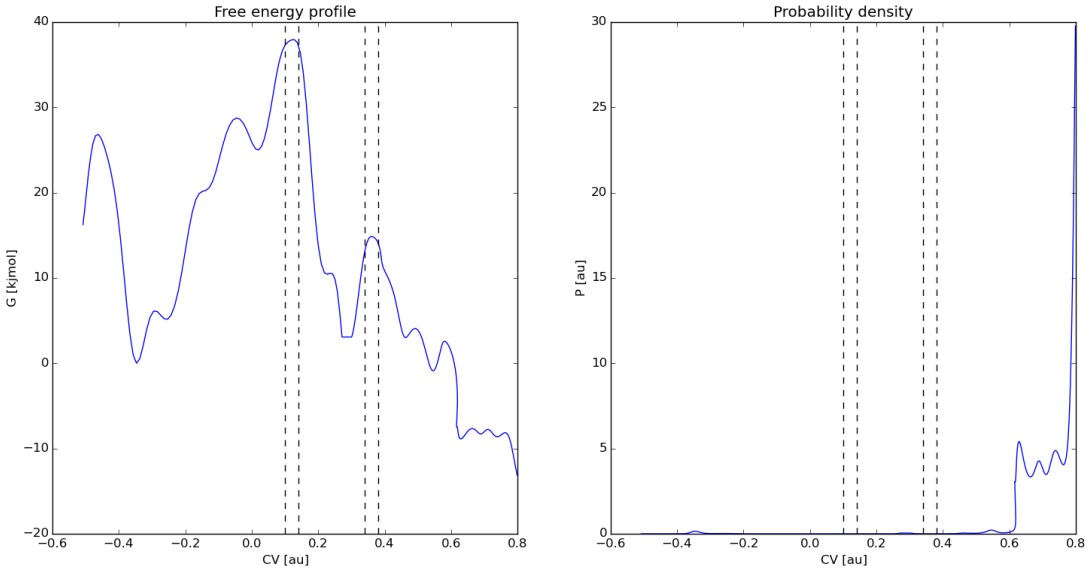

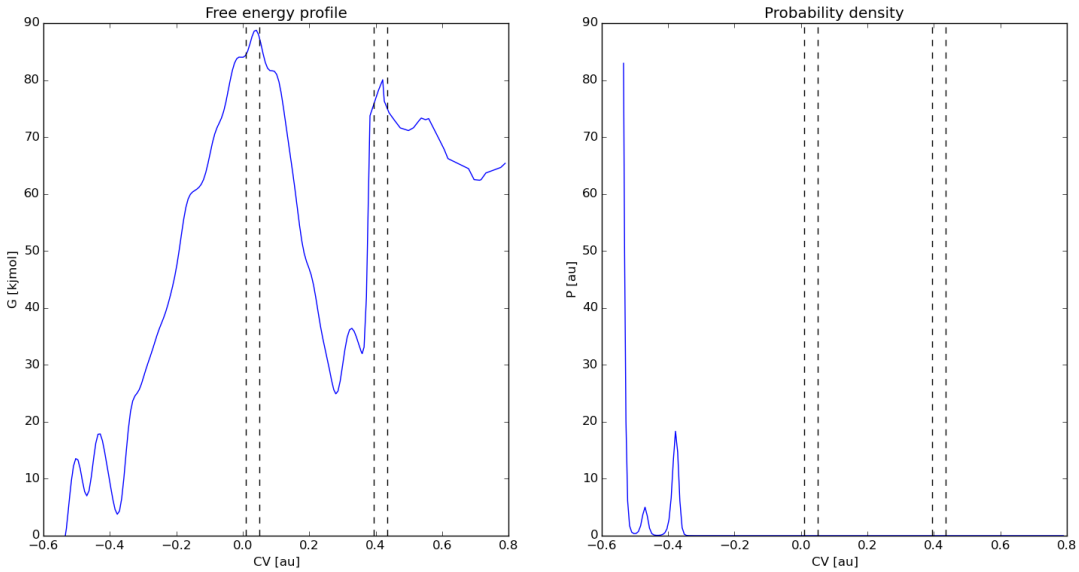

10.) metadynamics does not generate an equilibrium ensemble and hence the analysis of average geometric parameters (bottom paragraph on page 11) is completely irrelevant

This is true and we notice it in the manuscript.

11.) Fig. 5 and Tab. 1 show that the free-energy difference between the 2-pentoxide and the physisorbed species is slightly negative but that for 3-pentoxide is highly positive (~50 kJ/mol). On p. 13, the authors provide the following explanation: "The formation of 3-pentoxide is less probable, a higher free energy of activation is found and the formed 3-pentoxide is less stable than the other alkoxides. This observation is systematically found for all methodologies used in this work, and is probably due to unfavorable steric interactions with the walls of the zeolite." If this were true, there should be a significant difference in finite-T enthalpies between physisorbed and chemisorbed species but this is clearly not the case, see Fig. 4 (reference to 0K calculations is quite irrelevant here because the thermal effect included in MTD calculations is of the same quality as that in conventional MD). The authors should provide better explanation for the apparent inconsistency

between these MD and MTD results.

This is an interesting question and the apparent inconsistency between MD and MTD for 3-pentoxide can be due to multiple factors. Before the deprotonation of the BAS takes place (before climbing up TS1) , the free energy profile shows local bumps and local minima which may probably be ascribed to a repositioning of the π-complex relative to the zeolite lattice to bring the adsorbate in the correct position for the formation of the carbenium ion structure. In addition there are a lot of constraints imposed in the MTD run for the formation of the pentoxide. Standard MD simulations don't cross barriers. We performed MD simulations on the pentoxides and extracted the ensemble average enthalpic energies. To correlate MD results with MTD outcome we need several MD simulations starting with different initial structures, etc. Although a very interesting issue, this is not the scope of the paper. In addition, the free energies resulting from a MTD simulation don't allow a partition between enthalpic and entropic contributions. What we mainly learn after inspecting the three free energy profiles is that the third reaction transforming 2-pentene to 3-pentoxide behaves

dramatically different with a deep and broad metastable state for the 3-pentyl intermediate surrounded by two transition states, which both are high in energy : the formation of the 3-pentyl intermediate requires almost ~ 85 kJ/mol, while more than 50 kJ/mol is needed to overcome the next barrier to form the 3-pentoxide product, which is more than 35 kJ/mol higher than for the pentoxide formation in the former two reactions. We ascribe this apparent difference to steric interactions that the 3-pentyl and 3-pentoxide feel with the walls of the zeolite. MD simulations have revealed that by preference the shortest tail of the chemisorbed pentoxide is oriented in the zigzag channel. For a 2-pentoxide it is a methyl end that enters the channel, while for a 3-pentoxide it is a propyl group (we refer to Figure 4 of the revised manuscript for the visualization) encountering more interaction with the wall.

1. De Moor, B.A., et al., *Adsorption of C2-C8 n-Alkanes in Zeolites.* Journal of Physical Chemistry C, 2011. **115**(4): p. 1204-1219.
2. Piccini, G., et al., *Accurate Adsorption Thermodynamics of Small Alkanes in Zeolites. Ab initio Theory and Experiment for H-Chabazite.* Journal of Physical Chemistry C, 2015. **119**(11): p. 6128-6137.
3. Jiang, T., et al., *Effect of Temperature on the Adsorption of Short Alkanes in the Zeolite SSZ-13-Adapting Adsorption Isotherms to Microporous Materials.* Acs Catalysis, 2014. **4**(7): p. 2351-2358.
4. Goltl, F. and J. Hafner, *Alkane adsorption in Na-exchanged chabazite: The influence of dispersion forces.* Journal of Chemical Physics, 2011. **134**(6): p. 064102.
5. Gomes, J., et al., *Accurate Prediction of Hydrocarbon interactions with Zeolites Utilizing improved Exchange-Correlation Functionals and QM/MM Methods: Benchmark Calculations of Adsorption Enthalpies and Application to Ethene Methylation by Methanol.* Journal of Physical Chemistry C, 2012. **116**(29): p. 15406-15414.
6. Dai, W.L., et al., *Identification of tert-Butyl Cations in Zeolite H-ZSM-5: Evidence from NMR Spectroscopy and DFT Calculations.* Angewandte Chemie-International Edition, 2015. **54**(30): p. 8783-8786.
7. Tuma, C. and J. Sauer, *Protonated isobutene in zeolites: tert-butyl cation or alkoxide?* Angewandte Chemie-International Edition, 2005. **44**(30): p. 4769-4771.
8. Van der Mynsbrugge, J., et al., *Insight into the Formation and Reactivity of Framework-Bound Methoxide Species in H-ZSM-5 from Static and Dynamic Molecular Simulations.* Chemcatchem, 2014. **6**(7): p. 1906-1918.
9. Moors, S.L.C., et al., *Molecular Dynamics Kinetic Study on the Zeolite-Catalyzed Benzene Methylation in ZSM-5.* Acs Catalysis, 2013. **3**(11): p. 2556-2567.
10. De Wispelaere, K., et al., *Complex Reaction Environments and Competing Reaction Mechanisms in Zeolite Catalysis: Insights from Advanced Molecular Dynamics.* Chemistry-a European Journal, 2015. **21**(26): p. 9385-9396.
11. Wellendorff, J., et al., *Density functionals for surface science: Exchange-correlation model development with Bayesian error estimation.* Physical Review B, 2012. **85**(23): p. 235149.

*Graphical Abstract (for review)

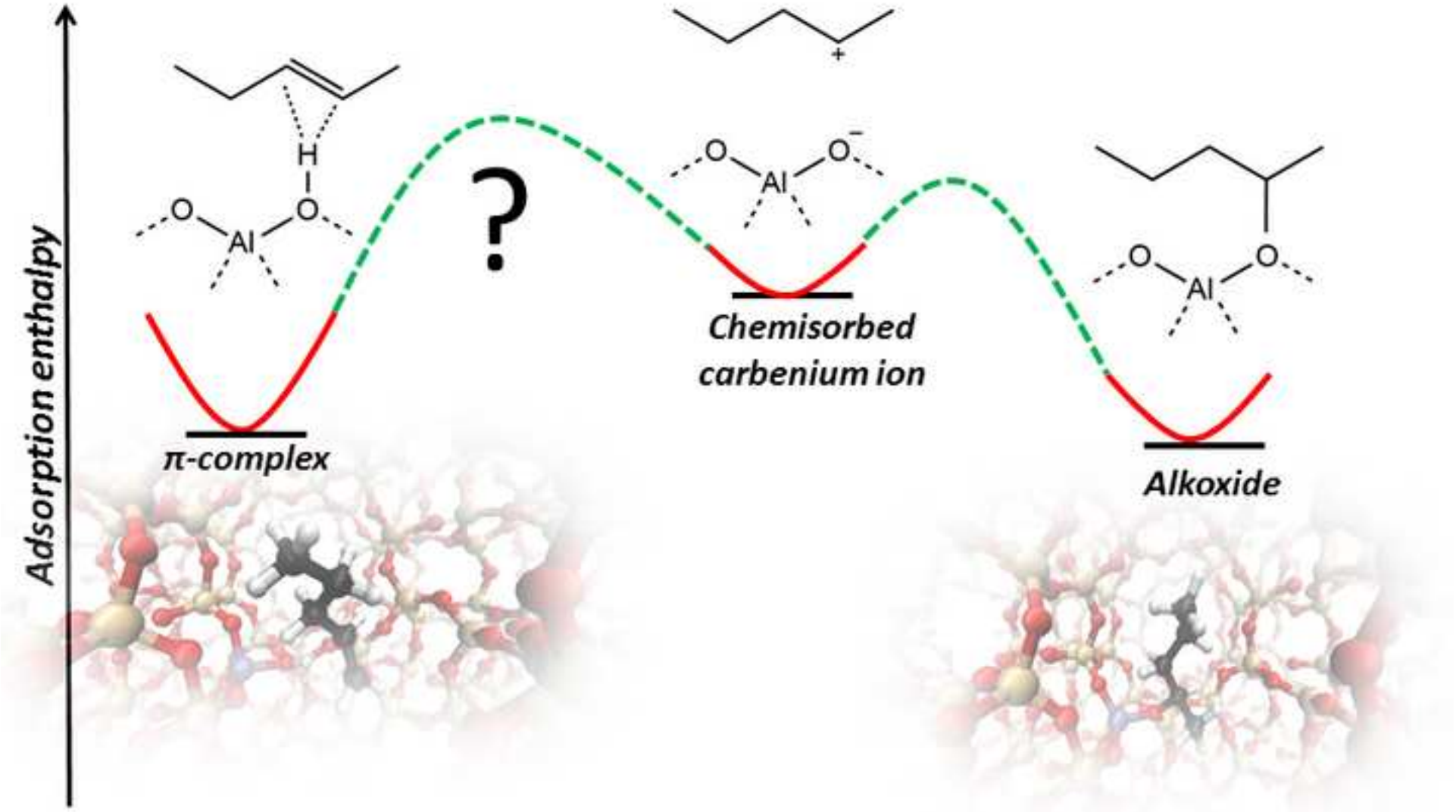

Highlights

- Adsorption of linear pentenes in H-ZSM-5 at 323 K yield an almost equally stable π-complex and covalently bound alkoxide
- The transformation from the π-complex to the chemisorbed complex is activated by a free energy in the range of 33-42 kJ/mol
- The stability has been unravelled by contemporary static and dynamic first principle methods
- Theoretical calculations can predict the stability of elusive and reactive intermediates in zeolite catalysis

*Manuscript
Click here to view linked References

On the stability and nature of adsorbed pentene in Brønsted acid zeolite H-ZSM-5 at 323 K

*J. Hajek , J. Van der Mynsbrugge, K. De Wispelaere , P. Cnudde, L. Vanduyfhuys, M. Waroquier and V. Van Speybroeck**

Center for Molecular Modeling, Ghent University, Technologiepark 903, B-9052 Zwijnaarde, Belgium

*Corresponding author:

veronique.vanspeybroeck@ugent.be

ABSTRACT: Adsorption of linear pentenes in H-ZSM-5 at 323 K is investigated using contemporary static and molecular dynamics methods. A physisorbed complex corresponding to free pentene, a π-complex and a chemisorbed species may occur. The chemisorbed species can either be a covalently bonded alkoxide or an ion pair, a so-called carbenium ion. Without finite temperature effects, the π-complex is systematically slightly more bound than the chemisorbed alkoxide complex, whereas molecular dynamics calculations at 323 K yield an almost equal stability of both species. The carbenium ion was not observed during simulations at 323 K. The transformation from the π-complex to the chemisorbed complex is activated by a free energy in the range of 33-42 kJ/mol. Our observations yield unprecedented insights into the stability of elusive intermediates in zeolite catalysis, for which experimental data are very hard to measure.

1. Introduction

Solid acids such as zeolites are widely applied in the chemical industry for conversion of hydrocarbons in reactions such as catalytic cracking, hydrocracking and alkylation.[1-6] These reactions involve alkanes and alkenes as reactants and products which interact with the zeolite and its Brønsted acid sites (BAS).[7] The understanding of alkane adsorption on various zeolites has been the subject of numerous experimental studies, whereas comparatively little is known about adsorption of alkenes, due to their high reactivity even at low temperatures. [8-10]

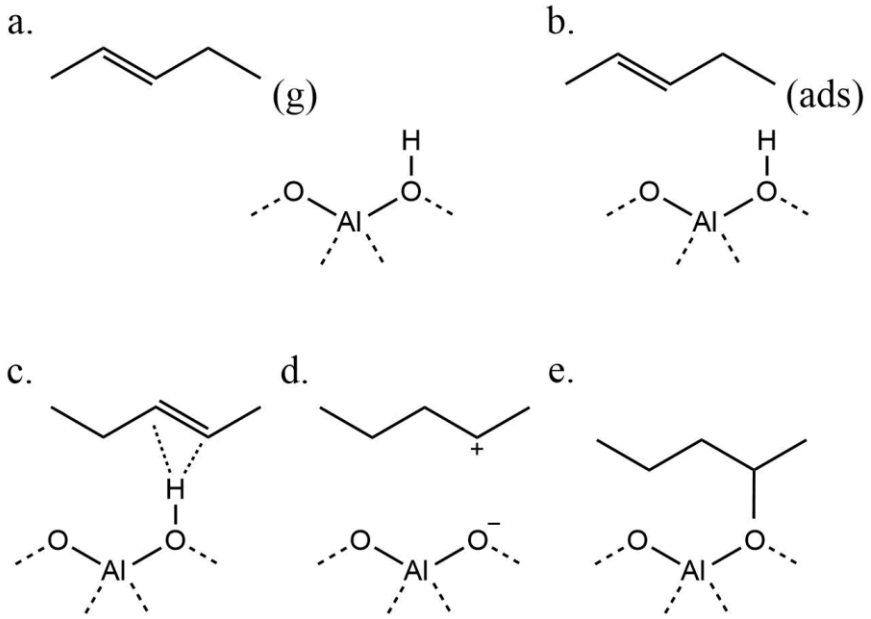

Figure 1: Illustration of the different intermediates upon alkene (2-pentene) adsorption in the presence of a Brønsted acid site (BAS): (a) alkene in gas phase, (b) alkene physisorbed in the channels of the zeolite (c) alkene π-complex, (d) chemisorbed carbenium ion (e) chemisorbed alkoxide.

When an alkene adsorbs on a Brønsted acid zeolite, various adsorbed species may be distinguished as schematically indicated in Figure 1. [11-14] A first state corresponds to a free alkene in the cages of the zeolite, which undergoes only a weak van der Waals (vdW) interaction with the walls of the zeolite. This state is further referred to as the physisorbed state. A more bound state corresponds to the π-complex, where a specific non-bonded interaction between the π-electrons of the double bond and the Brønsted acid site occurs. Finally the π-complex may be protonated leading to the formation of a chemisorbed species. [11-14] The nature of the resulting intermediate is still debated. It has been proposed to be stabilized as a covalently bonded alkoxide or as an ion pair which is referred to as a free carbenium ion (Figure 1). [11, 12, 15-17]

Alkene adsorption is very difficult to track experimentally as these hydrocarbons are highly reactive even at low temperatures. Solely based on experiment it is practically excluded to gain insight into the nature of the adsorbed complexes and intermediates, which can be very short-lived. For butenes some NMR and infrared based adsorption studies are available. The adsorption of butenes on H-ZSM-5 and mordenite was experimentally investigated by Domen et al. [12, 13, 17-19] On H-ZSM-5, they observed that at sub-ambient temperatures a stable π-complex was formed and that double bond isomerization occurred already at 230 K. [13, 18, 20] A concerted mechanism was suggested to explain the rapid double bond isomerization despite the absence of a classical carbenium ion at these temperatures, as evidenced from isotope experiments.[20-22] Isotope experiments evidenced in addition the high mobility of alkenes already at sub-ambient

temperatures. [18, 20] Stepanov et al. studied the kinetics of the double-bond shift reaction, H/D exchange and ^{13}C scrambling for linear butenes on FER by means of ^{1}H, ^{2}H and ^{13}C MAS NMR for temperatures above 290 K and determined activation energies for the double bond shift and showed that carbenium ions are involved in the mechanism of double bond isomerization at higher temperatures. [21, 23]

Due to the lack of experimental data, theoretical studies are indispensable to obtain insight into the nature and stability of adsorbed species. Adsorption of alkanes has been studied extensively in literature by various theoretical methods. A more complete literature overview may be found in some recent reviews. [24, 25] For alkenes much less information is available also from a theoretical point of view. In a series of papers by Sauer and co-workers various theoretical methods were used to study the adsorption behavior of C4 species in H-FER. [26, 27] The methods varied in the treatment of the molecular environment, the method to account for the long range dispersion interactions and the degree to which finite temperature effects were accounted for. All three factors are decisive to determine the relative stabilities of the π-complex, carbenium ions and alkoxide species. The stability of carbenium ions not only depends on the carbon skeleton, i.e. secondary, tertiary, cyclic, but also largely on the applied temperature. Higher temperatures may favor the existence of persistent carbenium ions. Nicholas and Haw concluded that stable carbenium ions could be observed by NMR provided that the neutral compound from which it originates has a proton affinity of 875 kJ mol^{-1} or larger.[28] However the topology of the material may also be very important as was shown by Fang et al. [29, 30] It was only very recently that the tert-butyl cation on H-ZSM-5 was identified by capturing this reaction intermediate with an ammonia molecule and by identifying the stable surface compounds by $^{1}H/^{13}C$ magic angle spinning NMR spectroscopy and density functional theory calculations. [31] The physisorption and chemisorption of alkenes beyond C4 in a variety of zeolites (H-FAU, H-BEA, H-MOR, H-ZSM-5) was studied by Marin and co-workers using the QM-Pot methodology originally developed by Sauer and co-workers. [14, 32, 33] The method relies on a combination of a quantum mechanics approach on a smaller part of the system combined with an interatomic potential approach on the periodic structure. The QM-Pot methodology has proven very valuable in the time frame where periodic static calculations with more advanced functionals and dispersion interactions were unfeasible. Some earlier theoretical works also reported on the relative stabilities of alkenes, but this was done in absence of dispersion interactions, however also the importance of various rotational orientations of the adsorbed species was emphasized. [11] Indeed Göltl and co-workers stressed the role of finite temperature effects and mobility of adsorbed species in case of alkanes. For methane, ethane and propane in protonated chabazite at 300 K there was a substantial probability that the adsorbate desorbs from the acid site and moves freely in the pores of the zeolite, yielding adsorption enthalpies which are systematically smaller than the prediction at 0 K. [34, 35]

To the best of our knowledge no experimental data are available for alkene adsorption in H-ZSM-5 beyond C4. Furthermore no fully periodic density functional theory calculations are available for the various adsorbed species of alkenes higher than C4, neither from static calculations at 0 K nor from molecular dynamics calculations to account for finite temperature effects on the adsorption behavior. Such understanding is however crucial to optimize industrially important processes such as olefin cracking. These processes receive a lot of interest to selectively produce propene, by cracking less valuable C_4 through C_8 olefins. [36-38] Alkene cracking processes consist of a complex reaction network including isomerizations, oligomerizations, alkylations, hydride transfers and cracking reactions. [3, 7, 39] In any case, knowledge on the reaction intermediates is of utmost importance.

In this paper we present a complete study on the adsorption behavior of linear pentenes in H-ZSM-5, which is one of the most effective industrial catalysts in light olefin production due to its optimal balance between conversion, selectivity and coke formation stability. [40-42] The applied methodology encompasses static periodic density functional theory calculations using contemporary density functionals and methods to account for the dispersion interactions, first principle molecular dynamics simulations at 323 K to account for the mobility of the adsorbates, and metadynamics simulations to sample the transformations among π-complex, alkoxide and carbenium ion and to deduce the corresponding free energy barriers. This complementary set of tools provides an overall picture of the various adsorbed species in the absence of current relevant experimental data. Such insights into the relative stability of adsorbed species is of fundamental importance for our understanding of zeolite catalysis.

2. Computational Methods

H-ZSM-5 was represented by a periodic model to fully account for the zeolitic surroundings (Figure S.1 of the SI). Static periodic Density Functional Theory (DFT) calculations were performed with the Vienna Ab Initio Simulation Package (VASP 5.3). [43-46] Initial geometries were constructed with ZEOBUILDER. [47] The position of the Brønsted acid site (BAS) is the same as in earlier works of the authors [24, 48] with a substitutional aluminum at the T12 position of the orthorhombic MFI unit cell and the charge compensating proton on O_{20} , resulting in a BAS at the intersection of the straight and sinusoidal channels (Figure S.1). All structures were first optimized with a PBE functional using Grimme D3 dispersion corrections. [49] During the calculations the projector augmented approximation (PAW) [50, 51] together with a plane wave kinetic energy cutoff of 600 eV were used and sampling of the Brillouin zone was restricted to the Γ-point. The convergence criterion for the electronic self-consistent field (SCF) problem was set to 10^{-5} eV. For all static

periodic DFT calculations the unit cell was relaxed during the geometry optimizations. Afterward, the energy was refined with a variety of exchange correlation functionals and dispersion models encompassing revPBE-D3 with and without Becke Johnson damping (BJ) [52], revPBE with the non-local correlation functional vdW-DF of Dion [53], BEEF-vdW [54], and PBE with the new many body dispersion (MBD) scheme of Tkatchenko with conventional (MBD-vdW_H) and iterative Hirshfeld partitioning (MBD-vdW_HI). [55, 56] The thermal corrections were performed on the basis of frequencies obtained with a partial Hessian approach including 8T atoms, the acid proton and the adsorbate. De Moor et al. [8] demonstrated that this type of procedure of using a partial Hessian is sufficient to determine accurate enthalpy and entropy differences. The nature of the local minima was verified by a normal mode analysis and the obtained partial Hessian matrix included only positive eigenmodes. We applied the partial Hessian vibrational analysis (PHVA) [55–57] as implemented in an in-house post-processing toolkit TAMkin. [57]

Ab initio molecular dynamics (MD) simulations were performed with the CP2K software package [58] on the DFT level of theory by using the combined Gaussian Plane Wave basis sets approach. [59, 60] The revPBE-D3 functional [61] together with the DZVP-GTH basis set and pseudopotentials were chosen. [62] This combination of exchange correlation functional and dispersion model was successfully used in earlier zeolite catalysis work. [48, 63, 64] Since ab initio molecular dynamics calculations performed on the complete zeolite model are computationally very expensive, more advanced methods using hybrid functionals or many body dispersion models are not feasible for simulations of considerable time length as emphasized here. [65, 66] The cell parameters were determined from a preliminary NPT run on the empty zeolite unit cell at 323K and 1 atm and are found to be a = 20.14 Å, b = 20.33 Å, c = 13.56 Å, α = 89.82 °, β = 89.47 °, γ = 90.15°. Subsequent molecular dynamics and metadynamics (cf. infra) simulations on the various complexes were performed in the NVT ensemble at 323K. The integration time step was set to 0.5 fs. The temperature was controlled by a chain of five Nosé-Hoover thermostats. [67] The MD simulations also allow the computation of finite-temperature adsorption enthalpies for the various π-complexes and alkoxides from ensemble averages of the internal energies over the MD trajectories from separate simulations on the complex, the empty zeolite and the adsorbate in gas phase. More details on the procedure and the influence of the length of the MD runs are given in the SI.

To accelerate sampling of the activated transition from the π-complex to the pentoxide and to explore the nature of the carbenium ion, a metadynamics (MTD) approach was employed. [68, 69] This method has recently been applied successfully in various zeolite catalysis studies. [63, 70] During an NVT MTD run with similar settings as for the MD simulations, Gaussian hills are added every 25 fs along two collective variables (CVs), described by coordination numbers (CN), which are able to describe the reaction coordinate for

transformations between the various adsorbed species. The first CV is defined by CN(H-O) – CN(H-C1) and describes the proton transfer from the zeolite to the pentene; the second CV is defined by CN(C2-Oz) and describes the formation of the C-O bond between the resulting pentyl carbenium ion and the zeolite framework. C1 and C2 are the carbon atoms forming the double bond and visualized in **Figure 2** together with the definition of the collective variables. The metadynamics simulations yield a two-dimensional free energy surface in terms of the two collective variables. A 1D free energy profile is constructed by projecting the 2D free energy onto the minimum free energy path after which the free energy of activation may be computed. [71] More technical details of the simulations are taken up in the SI.

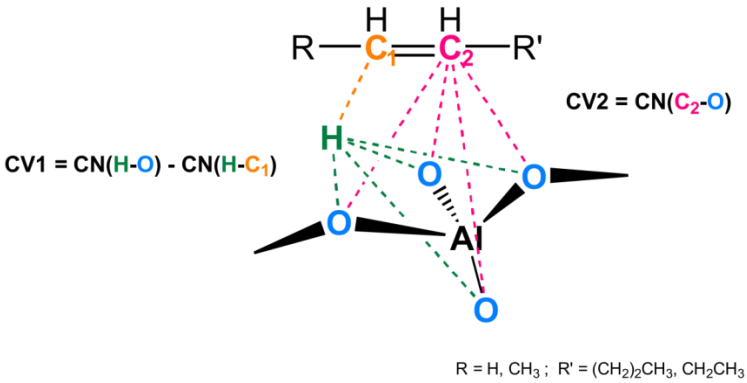

Figure 2: Schematic visualization of the collective variables used for the various metadynamics simulations.

3. Results and discussion

To obtain insight into the mobility of the various adsorbed pentene species and the various plausible configurations, a series of ab initio MD runs were performed at 323 K on 1-pentene (π), 2-pentene (π), 2-pentoxide and 3-pentoxide complexes. As the potential energy surface (PES) contains a large number of local minima, we first performed a number of short MD runs of about 10 ps starting from an unbiased initial position corresponding to an orientation of the physisorbed pentene molecule in the center of the straight 10-membered ring cavity at about 4 Å from the acid site. We followed how the 2-pentene evolved during the initial stages of the simulation. In the Supporting Information we display some snapshots. The adsorbate which only interacts with the walls of the zeolite, quickly diffuses towards the acid site to form the π-complex. The 2-pentene molecule is preferentially positioned with the methyl end directed in the sinusoidal channel near the BAS and the longer ethyl tail in the straight cavity. These initial MD runs are then followed by more extensive production molecular dynamics runs of 100 ps starting from the optimal configuration obtained from the initial MD runs. The π-complex is characterized by the distance between the C=C double

bond and the acid proton (H_z). The probability distribution of the shortest distance between one of the carbon atoms in the double bond and the acid proton during the simulation is plotted in **Figure 3**. For both 1- and 2-pentene the shortest C-H_z distance is on average about 2 Å, indicating that the π-H interaction remains in place throughout the simulation. During the simulations at 323 K we did not observe the carbenium ion. For the alkoxides a similar analysis was done, yielding average C-O_z distances of about 1.6 Å, indicating that these complexes also remain stable during the simulation.

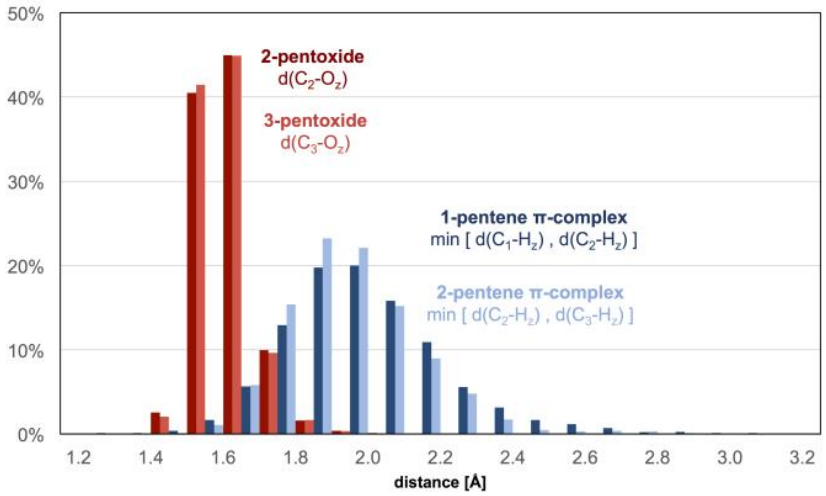

Figure 3: Probability distributions of some critical distances in molecular dynamics simulations of π-complexes and alkoxides in H-ZSM-5 obtained over a 60 ps run. Min[d(C_1-H_z),d(C_2-H_z)] stands for the shortest C-H_z distance in 1-pentene π-complex [average 2.07 Å]; Min[d(C_2-H_z),d(C_3-H_z)] stands for the shortest distance in the 2-pentene π-complex [average : 2.04 Å]; d(C_2-O_z) is the C_2-O_z distance in 2-pentoxide complex [average: 1.62 Å]; and d(C_3-O_z) is the C_3-O_z distance in 3-pentoxide complex [average: 1.62 Å].

Besides geometrical features MD simulations also release information about adsorption enthalpies. They are discussed further in the text where we investigated the influence of finite temperature effects on the adsorption process. First we report the 0 K results predicted by static calculations for the most visited structures.

In a next step, based on the probability distribution (Figure 3) we determined adsorption positions corresponding to the most frequently visited structures during the MD runs and performed static calculations on these initial structures to get the optimized geometries. Subsequent frequency calculations lead finally to the adsorption enthalpies. For 1- and 2-pentene the energetically favorable configuration corresponds to the

adsorbate positioned in straight channel with its methyl tail oriented into the zigzag channel. The most plausible structures are visualized in Figure 4. To ensure that the selected geometries for the static calculations do not substantially influence the obtained energetics, additional geometry optimizations were performed on a range of other geometries also generated from MD simulations. More details are taken up in Section 3.1 of the SI.

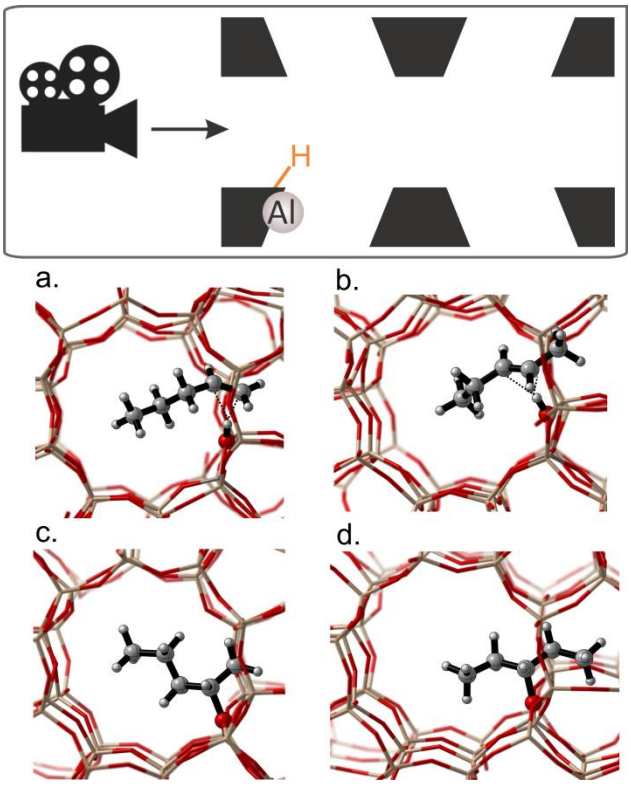

Figure 4: MD snapshots of a) 1-pentene π-complex, b) 2-pentene π-complex, c) chemisorbed 2-alkoxide, d) chemisorbed 3-alkoxide in H-ZSM-5 at 323K, seen in the direction of the straight channel (camera viewpoint). The snapshots correspond to geometries which are most frequently visited during MD runs of 100 ps at 323 K.

A decisive parameter for the energetics of the adsorbed species is the distance of the carbon skeleton with respect to the BAS. After optimization, the 1-pentene π-complex has a characteristic shortest C-H_z distance of about 1.9 Å. For 2-pentene π-complex this is about 2 Å. The pentoxide species are characterized by a C-O_z distance of about 1.6 Å . In order to check the influence of different functionals and dispersion models, we refined the energies using revPBE [53] and BEEF [54] functionals. Also some recently introduced dispersion models were tested such as the models of Tkatchenko et al. [55, 56] An overview of the adsorption enthalpies and free energies is given in Table S.3 of the SI. All applied level of theories (LOT's) systematically predict the π-complexes more stable with respect to their chemisorbed counterparts by some

15-30 kJ/mol. The qualitative trends remain the same for all used levels of theory. The results show that the Becke-Johnson (BJ) damping function [52], revPBE-vdW-DF and BEEF-vdW levels of theory, even substantially enlarge the stability of the π-complexes compared with all other dispersion models, which indicates that these methods predict an overbinding of the adsorbed species.

Table 1: Free energy ΔG and enthalpy ΔH differences for configurations for the π-complex and chemisorbed complex in H-ZSM-5 at 323 K. All energies in kJ/mol. Use of the standard notation "LOT-E"//"LOT-G" (LOT-E and LOT-G being the electronic levels of theory used for the energy and geometry optimizations, respectively).

	PBE-D3 //PBE- D3		revPBE-D3 //PBE- D3		revPBE-D3(BJ) //PBE D3		revPBE-vdW-DF //PBE D3		BEEF-vDW //PBE D3		PBE-MBD-vdW_H//PBE D3		PBE-MBD-vdW_HI//PBE D3	
	ΔG	**ΔH**	**ΔG**	**ΔH**	**ΔG**	**ΔH**	**ΔG**	**ΔH**	**ΔG**	**ΔH**	**ΔG**	**ΔH**	**ΔG**	**ΔH**
1-pentene (g) -> 1-pentene (π)	-45.0	-103.2	-58.4	-116.6	-76.1	-134.3	-106.7	-164.9	-68.4	-126.6	-51.3	-109.5	-39.9	-98.1
2-pentene (g) -> 2-pentene (π)	-52.7	-109.6	-73.3	-130.2	-90.7	-147.6	-112.4	-169.2	-71.1	-128.0	-58.6	-115.5	-44.7	-101.6
1-pentene (g) -> 2-pentoxide	-17.5	-84.9	-40.1	-107.5	-60.3	-127.8	-69.2	-136.6	-29.4	-96.8	-30.6	-98.0	-15.0	-82.5
2-pentene (g) -> 2-pentoxide	-4.1	-72.2	-28.7	-96.8	-47.4	-115.6	-58.2	-126.4	-17.8	-86.0	-17.2	-85.3	-1.4	-69.6
2-pentene (g) -> 3-pentoxide	-3.0	-68.8	-21.3	-87.1	-39.8	-105.6	-52.9	-118.7	-14.1	-80.0	-19.9	-85.7	-2.8	-68.6
1-pentene (π) -> 2-pentoxide	27.5	18.3	18.3	9.1	15.8	6.6	37.6	28.3	39.0	29.8	20.7	11.5	24.9	15.7
2-pentene (π) -> 2-pentoxide	48.6	37.4	44.6	33.3	43.3	32.0	54.1	42.8	53.3	42.0	41.4	30.1	43.3	32.0
2-pentene (π) -> 3-pentoxide	49.7	40.8	52.0	43.0	50.9	42.0	59.5	50.5	57.0	48.0	38.7	29.8	41.9	33.0

Göltl and co-workers reached similar conclusions for the revPBE-vdW-DF method and an in depth analysis was presented more recently by Göltl and Sautet. [72]

To investigate also the influence of the level of theory on the geometry optimization and the derived relative stabilities of the π-complex and alkoxide structures, we also performed new geometry optimizations and frequency calculations for 2-pentene π- complex and 2-pentoxide using the BEEF-vdW functional [54]. Geometrical details of the structures with PBE-D3 and BEEF-vdW functionals are given in **Table S.4**. There are no essential features which are different, but the most crucial result is that the free energy and the adsorption enthalpy differences for the π-complex and chemisorbed complex are very similar to each other (see **Table 2**) confirming our conclusions for the static calculations.

Table 2 : Free energy ΔG and enthalpy ΔH differences for configurations for the π-complex and chemisorbed complex in H-ZSM-5 at 323 K given in kJ/mol.

	BEEF-vdW //PBE D3		BEEF-vdW // BEEF-vdW	
	ΔG	**ΔH**	**ΔG**	**ΔH**
2-pentene (π) -> 2-pentoxide	53.27	41.96	51.05	42.7

Our theoretical findings give qualitatively and quantitatively different results than the values of Nguyen et al. produced with the QM-Pot methodology. [14] Recently, also Rosch et al. found similar deviating behavior for alkanes between periodic DFT and QM-Pot results. [73] A proper analysis of possible ingredients lying on the origin of the observed differences, learns that the deviancies should not be ascribed to the QM-Pot methodology itself, but mainly to less favorite geometries of the adsorbed species and their positions in the cavity. In the case studied by Nguyen et al. [14], the double bond of 1- and 2-pentene was located at about 2.3 Å from the BAS, which is significantly larger than the distances predicted in this work. The PES around the adsorption site was explored in a 4T cluster embedded in the zeolite unit cell, and is by far not as accurate as the present calculations where the influence of the environment on the PES is intensively investigated in first-principles MD simulations of the periodic models. The geometries for 1- and 2-pentene reported in ref. [14] differ by far from the configurations obtained in this work. On the other hand the geometrical parameters of the corresponding pentoxides found in the two studies are completely similar, so that the difference in stability between the physisorbed and chemisorbed complexes must be ascribed to the position of the physisorbed pentene to the BAS. This is an important statement as it reduces the discussion on the

exothermic or endothermic character of the chemisorption process to the localization of the adsorbed pentene π-complex in the pores of the zeolite and more particularly the distance from the BAS.

In a next step, we assessed the influence of finite temperature effects on the adsorption enthalpies. The probability distributions for the distances of the various adsorbed species to the BAS, reveal an asymmetric behavior for the π-complexes towards higher C-H distances. For 1-pentene this is even more pronounced than for 2-pentene. The adsorption enthalpy of 1- and 2- pentene is strongly correlated with the C-H distance. The broad probability distribution for these two species clearly indicates that the average ensemble over the MD trajectories results in enthalpy of adsorption which corresponds to larger C-H distances than 2 Å. On the other hand, the static calculations only consider one point on the potential energy surface (that corresponds to the optimized geometry) and do not account for configurations with slightly larger distances as observed in the MD simulations. Indeed the dynamically averaged values for the adsorption enthalpies yield systematically lower adsorption enthalpies for the π-complexes and slightly larger values for the alkoxides. The adsorption enthalpies for the π-complexes are shifted with about 20 kJ/mol. **Figure 3** also reveals that the C-O_z distances in the pentoxides are more peaked around 1.6 Å with almost 80 % probability yielding slightly more bound adsorption enthalpies from MD simulations. The adsorption enthalpies of pentoxides obtained as an ensemble average in the MD simulations are closer to the values obtained with static approaches. If finite temperature effects are taken into account the π-complexes are almost equally stable as the alkoxide species. A summarizing adsorption enthalpy diagram is given in **Figure 5**. In good agreement with ref [11], the double bond position does not affect significantly the enthalpy of formation of the π-complex. Static calculations systematically overestimate the adsorption enthalpies for the π-complex, which is inherently related to the usage of optimized geometries, which are necessary to compute enthalpic and entropic contributions, but neglect the asymmetric probability distribution shown in **Figure 3** at finite temperatures.

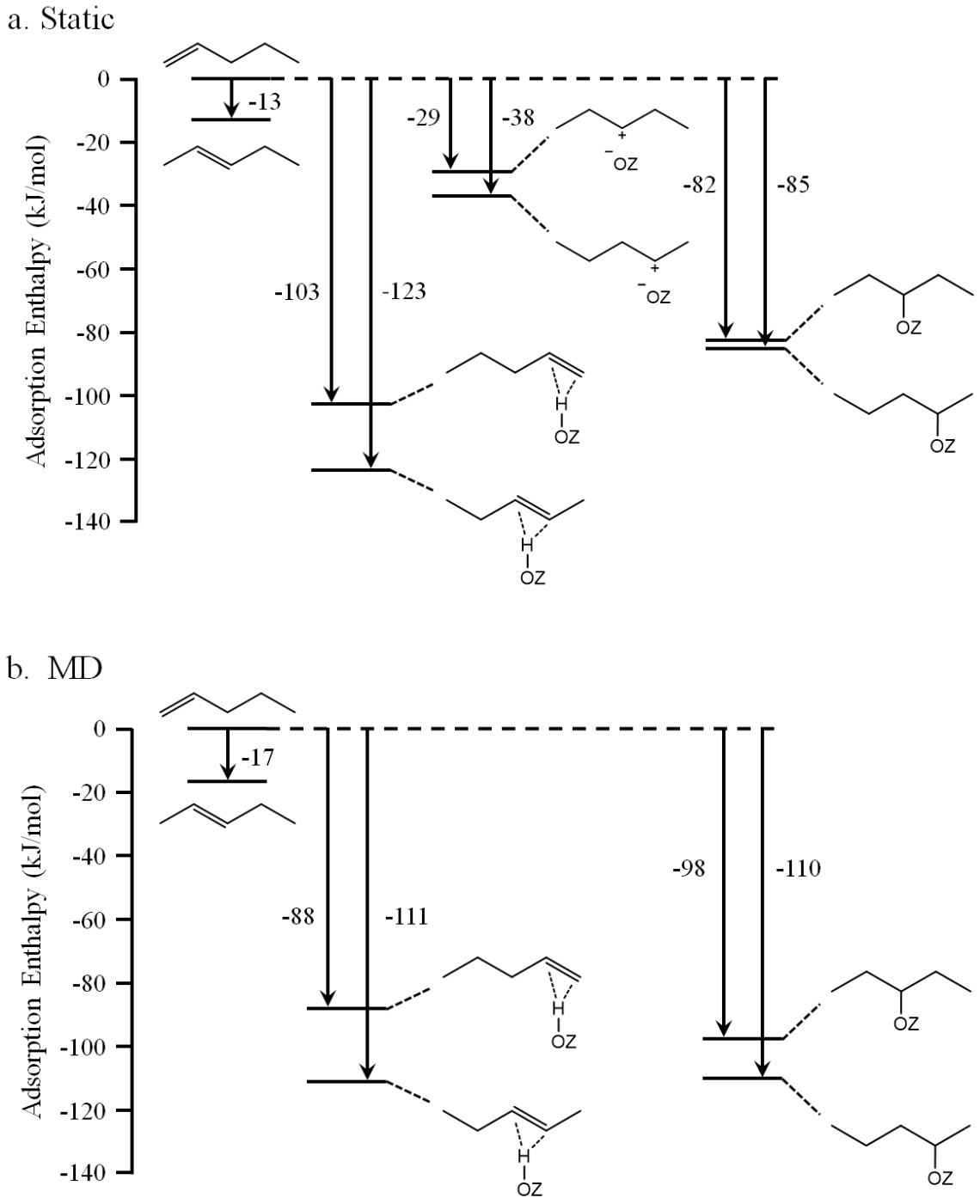

Figure 5. Adsorption enthalpy diagrams at 323 K for the several pentene intermediates with reference to 1-pentene in gas phase and an empty H-ZSM-5 framework, obtained from (a) static calculations at the PBE-D3 level (b) MD simulations at the revPBE-D3 level.

Finally we also wanted to investigate the possible occurrence of carbenium ions in the transition path from π-complexes to alkoxides. Therefore we used metadynamics simulations which allowed to sample the transition from the π-complex towards the chemisorbed species and to explore in how far the transformation is activated. Those simulations allow yielding detailed information on the nature of the chemisorbed species and the possible existence of a carbenium ion. In any case the carbenium ion was not observed during a regular MD run, nor was the transition from the π-complex towards the alkoxide seen, which points towards an activated transition.

The formation of 2-pentoxide from physisorbed 1-pentene and 2-pentene and that of 3-pentoxide from physisorbed 2-pentene were studied using metadynamics simulations with two collective variables to describe the reaction coordinate (cfr. Computational Methods). The resulting 2D free energy surfaces and 1D free energy profiles along the lowest free energy paths corresponding with the three reactions are displayed in **Figure 6**. There clearly exists a metastable state between the pentene π-complex and the pentoxide, which could be characterized as a carbenium ion. This metastable state mainly represents a 2-pentyl carbenium ion in the two reactions leading to 2-pentoxide; however, rapid isomerization to a 3-pentyl carbenium ion was observed as well.

In a next step the trajectories obtained from the metadynamics simulations were examined to distinguish between the free energy minima of the various adsorbed species. All samples in which the collective variable, corresponding to the coordination number representative for the C-O_z bond formation with the zeolite framework, is smaller than a cutoff value are identified as alkoxides. A similar procedure was applied for the identification of the pentyl carbenium ions. The detailed procedure is described in the SI. The procedure shows that it is possible to identify various basins corresponding to alkoxides where the C-O distance is on average 1.6 Å and corresponding to carbenium ions where the average distance is 3 Å, which is significantly larger than the value (2.0 Å) obtained with MD simulations for the π-complex (**Figure 3**). Here, some prudence should be taken into consideration as metadynamics does not generate an equilibrium ensemble and hence geometric parameters, given in MTD, are only indicative.

The 2D free energy surface is subsequently converted into a 1D free energy profile (by projection onto the minimum free energy path). For the three reactions under study the difference (CV2-CV1) of the two coordinations numbers turned out to be a good estimate for the one-dimensional reaction coordinate. The three free energy profiles for pentoxide formation, displayed in Figure 6, show the carbenium ion as a metastable intermediate between the π-complex and the alkoxide. They also allow to determine the free energy barriers ($\Delta G^{\ddagger}$) and reaction free energies (ΔG_r) between the various intermediate states following a procedure outlined in the SI. They are listed in Table 3.

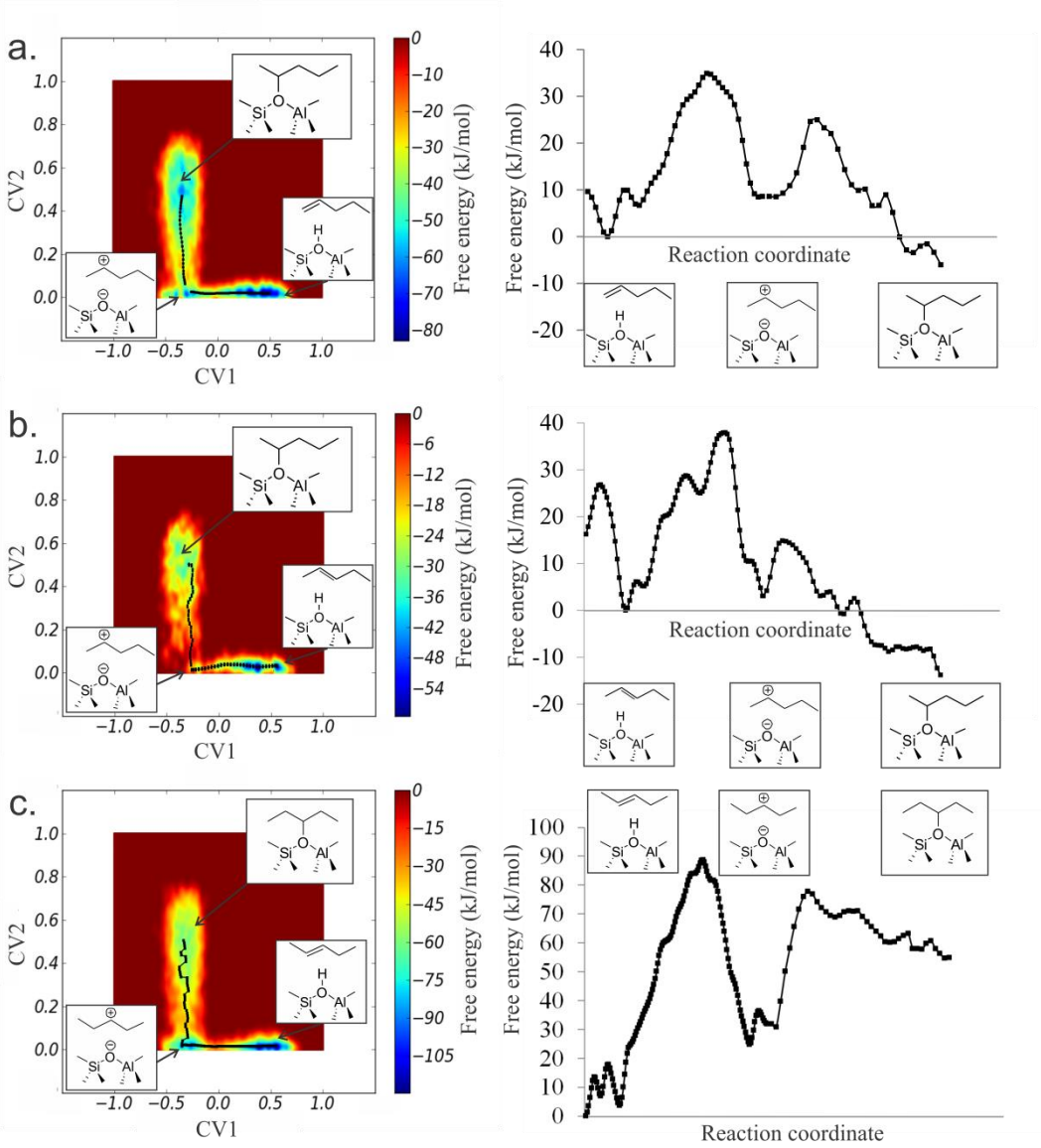

Figure 6. Left: 2D free energy surface for the formation of 2-pentoxide from a 1-pentene π-complex (a) or 2-pentene π-complex (b) and for the formation of 3-pentoxide from a 2-pentene π-complex (c) . The lowest free energy paths are displayed. A small well corresponding to the metastable carbenium ion can be observed in the bottom left corner. Right: corresponding 1D free energy profile along the lowest free energy path for the two reactions.

Table 3. Free energy barriers ($\Delta G^{\ddagger}$) and reaction free energies (ΔG_r) in kJ/mol at 323 K for the formation of a pentoxide from a pentene π-complex through a carbenium ion intermediate determined from MTD simulation in the NVT ensemble. LOT electronic energies: revPBE-D3/DZVP-GTH.

	$\Delta G^{\ddagger}$ (323 K) [kJ/mol]	**ΔG_r (323 K) [kJ/mol]**
1-pentene (π) → 2-pentyl carbenium	36.8	-2.3
2-pentyl carbenium → 2-pentoxide	20.3	-9.2
2-pentene (π) → 2-pentyl carbenium	38.2	+2.8
2-pentyl carbenium → 2-pentoxide	12.1	-15.2
2-pentene (π) -> 3-pentyl carbenium	84.7	+22.9
3-pentyl carbenium -> 3-pentoxide	54.6	+34.3

The observed free energy barriers for activation between the π-complex and the chemisorbed species largely vary from the type of the chemisorption process. The formation of 2-pentoxides is likely to occur at these temperatures as the free energy of activation corresponds to about 36.8 kJ/mol for 1-pentene to 2-pentyl carbenium ion and 38.2 kJ/mol for 2-pentene to 2-pentyl carbenium ion. The formation of 3-pentoxide is less probable, a higher free energy of activation is found and the formed 3-pentoxide is less stable than the other alkoxides. This observation is systematically found for all methodologies used in this work, and is probably due to unfavorable steric interactions with the walls of the zeolite. MD simulations have revealed that by preference the shortest tail of the chemisorbed pentoxide is oriented in the zigzag channel. For a 2-pentoxide it is a methyl end that enters the channel, while for a 3-pentoxide it is a propyl group (we refer to **Figure 4** for the visualization) encountering more interaction with the wall.

Apart from the formation of 3-pentoxide, the metadynamics simulations show that the alkoxide is only modestly more stable than the π-complex, which is in line with the earlier MD simulations.

Based on the metadynamics simulations, carbenium ions were observed and in a subsequent step these were also subjected to static periodic density functional theory calculations. When starting from configurations from the metadynamics simulations we could locate these highly elusive intermediates. The shortest C-O distance of the carbenium ion after this geometry optimization corresponds to 2.7 Å for the 2-pentyl carbenium ion and 3.4 Å for the 3-pentyl carbenium ion. The latter carbenium ion is further away from the BAS and is also about 10 kJ/mol less stable than the 2-pentyl carbenium ion. Based on the complementary set of simulations performed, we can now provide a full adsorption enthalpy diagram for all adsorbed species of 1-pentene and 2-pentene both from static and molecular dynamics simulations. This is visualized in **Figure 5** with all energy levels referred to the 1-pentene in the gas phase.

3. Conclusions

A complementary set of theoretical methods was used to fully characterize the adsorption behaviour of pentene in the pores of H-ZSM-5. Four distinct states of the olefin have been investigated: i) olefin adsorbed in the pores via dispersion forces, ii) interactions of the C=C bond of pentene with the Brønsted acid sites in the pores (π-complex), iii) the transient formation of a carbenium ion and iv) the stable formation of an alkoxide. The free physisorbed pentene was not observed during a substantial time of a molecular dynamics run at 323 K, instead a stable π-complex is rapidly formed, which does not transform towards alkoxides in a regular MD run but remains stable. This observation points towards an activated process to form stable chemisorbed species. The energies of π-complexes are very sensitive to the relative distance of the pentene molecule to the BAS. Adsorption enthalpies obtained from static calculations at 0K are systematically larger than dynamically averaged values, since only the optimized structure of the π-complex at 0 K is taken into account. Thermal fluctuations on the relative distance of the complex with the BAS give a better representation of the dynamical adsorption process and give adsorption enthalpies which are on average 20-30 kJ/mol less stable compared to their static values. Static periodic calculations have the advantage that they allow to use a large variation of DFT functionals and dispersion models. Göltl et al. observed same features for the adsorption behavior of alkanes and proposed to dynamically weight statically obtained adsorption enthalpies. [34] Based on our observations this might indeed be a good practice for future adsorption studies. Overall the π-complex and alkoxides (except the 3-pentoxide) are almost equally stable. To sample also the transformation between stable π-complexes and alkoxides the metadynamics technique was used. During the transformation we observed the carbenium ion, which seems to be a highly elusive intermediate. Furthermore the transformation from a π-complex to the carbenium ion is activated with a free energy of activation in the range of 32-36 kJ/mol in the most favorable cases. Starting from geometries taken from the metadynamics simulations we also determined the enthalpies of the carbenium ion, with static density functional theory calculations. It was confirmed that carbenium ions are transient species lying higher in energy.

Overall the present data offer a new platform for understanding the adsorption steps of olefins on zeolites in a quantitative manner, which will help, in turn, to better understand the intrinsic role of the strength of the Brønsted acid sites and the role of the local environment (siting of acid sites, available pore space) for the adsorption processes in the future.

Acknowledgments

JVdM, KDW, JH, PC, MW and VVS acknowledge the Fund for Scientific Research - Flanders (FWO), the Research Board of Ghent University (BOF), BELSPO in the frame of IAP/7/05 and the fund for scientific research Flanders (FWO) for financial support. VVS and KDW acknowledge funding from the European Union's Horizon 2020 research and innovation programme (consolidator ERC grant agreement No 647755 – DYNPOR (2015-2020)). The computational resources and services used in this work were provided by VSC (Flemish Supercomputer Center), funded by the Hercules foundation and the Flemish Government – department EWI. We would like to thank Prof. Johannes Lercher and Dr. Maricruz Sanchez-Sanchez (Department of Chemistry and Catalysis Research Center, Technische Universität München) for fruitful discussions.

References

[1] M. Guisnet, G. J.-P., Zeolites for Cleaner Technologies, Imperial College Press, London, 2002.
[2] A. Corma, Inorganic solid acids and their use in acid-catalyzed hydrocarbon reactions, Chemical reviews, 95 (1995) 559-614.
[3] J.S. Buchanan, J.G. Santiesteban, W.O. Haag, Mechanistic considerations in Acid-Catalyzed Cracking of Olefins, Journal of Catalysis, 158 (1996) 279-287.
[4] N. Rahimi, R. Karimzadeh, Catalytic cracking of hydrocarbons over modified ZSM-5 zeolites to produce light olefins: A review, Appl. Cat., A, 398 (2011) 1-17.
[5] P.A. Jacobs, J.A. Martens, In Introduction to Zeolite Science and Practice, Elsevier, Amsterdam, 1991.
[6] W. Vermeiren, J.P. Gilson, Impact of Zeolites on the Petroleum and Petrochemical Industry, Topics in Catalysis, 52 (2009) 1131-1161.
[7] Y.V. Kissin, Chemical mechanisms of catalytic cracking over solid acidic catalysts: Alkanes and alkenes, Catalysis Reviews-Science and Engineering, 43 (2001) 85-146.
[8] B.A. De Moor, M.F. Reyniers, O.C. Gobin, J.A. Lercher, G.B. Marin, Adsorption of C2-C8 n-Alkanes in Zeolites, J. Phys. Chem. C, 115 (2011) 1204-1219.
[9] F. Eder, J.A. Lercher, Alkane sorption in molecular sieves: The contribution of ordering, intermolecular interactions, and sorption on Brønsted acid sites, Zeolites, 18 (1997) 75-81.
[10] F. Eder, M. Stockenhuber, J.A. Lercher, Brønsted Acid Site and Pore Controlled Siting of Alkane Sorption in Acidic Molecular Sieves, The Journal of Physical Chemistry B, 101 (1997) 5414-5419.
[11] A. Bhan, Y.V. Joshi, W.N. Delgass, K.T. Thomson, DFT investigation of alkoxide formation from olefins in H-ZSM-5, Journal of Physical Chemistry B, 107 (2003) 10476-10487.
[12] H. Ishikawa, E. Yoda, J.N. Kondo, F. Wakabayashi, K. Domen, Stable dimerized alkoxy species of 2-methylpropene on mordenite zeolite studied by FT-IR, Journal of Physical Chemistry B, 103 (1999) 5681-5686.
[13] J.N. Kondo, S. Liqun, F. Wakabayashi, K. Domen, IR study of adsorption and reaction of 1-butene on H-ZSM-5, Catal. Lett., 47 (1997) 129-133.

[14] C.M. Nguyen, B.A. De Moor, M.-F. Reyniers, G.B. Marin, Physisorption and Chemisorption of Linear Alkenes in Zeolites: A Combined QM-Pot(MP2//B3LYP:GULP)-Statistical Thermodynamics Study, J. Phys. Chem. C, 115 (2011) 23831-23847.
[15] M. Boronat, P.M. Viruela, A. Corma, Reaction Intermediates in Acid Catalysis by Zeolites: Prediction of the Relative Tendency To Form Alkoxides or Carbocations as a Function of Hydrocarbon Nature and Active Site Structure, Journal of the American Chemical Society, 126 (2004) 3300-3309.
[16] V. Nieminen, M. Sierka, D.Y. Murzin, J. Sauer, Stabilities of C3–C5 alkoxide species inside H-FER zeolite: a hybrid QM/MM study, Journal of Catalysis, 231 (2005) 393-404.
[17] J.N. Kondo, F. Wakabayashi, K. Domen, IR Study of Adsorption of Olefins on Deuterated ZSM-5, The Journal of Physical Chemistry B, 102 (1998) 2259-2262.
[18] J.N. Kondo, K. Domen, F. Wakabayashi, Double bond migration of 1-butene without protonated intermediate on D-ZSM-5, Microporous Mesoporous Mat., 21 (1998) 429-437.
[19] E. Yoda, J.N. Kondo, K. Domen, Detailed Process of Adsorption of Alkanes and Alkenes on Zeolites, The Journal of Physical Chemistry B, 109 (2005) 1464-1472.
[20] J.N. Kondo, L. Shao, F. Wakabayashi, K. Domen, DoubleBond Migration of an Olefin without Protonated Species on H(D) Form Zeolites, The Journal of Physical Chemistry B, 101 (1997) 9314-9320.
[21] A.G. Stepanov, S.S. Arzumanov, M.V. Luzgin, H. Ernst, D. Freude, In situ monitoring of n-butene conversion on H-ferrierite by 1H, 2H, and 13C MAS NMR: kinetics of a double-bond-shift reaction, hydrogen exchange, and the 13C-label scrambling, Journal of Catalysis, 229 (2005) 243-251.
[22] M. Boronat, P. Viruela, A. Corma, Theoretical Study of the Mechanism of Zeolite-Catalyzed Isomerization Reactions of Linear Butenes, The Journal of Physical Chemistry A, 102 (1998) 982-989.
[23] A.G. Stepanov, M.V. Luzgin, S.S. Arzumanov, H. Ernst, D. Freude, n-Butene Conversion on H-Ferrierite Studied by 13C MAS NMR, Journal of Catalysis, 211 (2002) 165-172.
[24] V. Van Speybroeck, K. De Wispelaere, J. Van der Mynsbrugge, M. Vandichel, K. Hemelsoet, M. Waroquier, First principle chemical kinetics in zeolites: the methanol-to-olefin process as a case study, Chem. Soc. Rev., 43 (2014) 7326-7357.
[25] V. Van Speybroeck, K. Hemelsoet, L. Joos, M. Waroquier, R.G. Bell, C.R.A. Catlow, Advances in theory and their application within the field of zeolite chemistry, Chem. Soc. Rev., 44 (2015) 7044-7111.
[26] C. Tuma, T. Kerber, J. Sauer, The tert-Butyl Cation in H-Zeolites: Deprotonation to Isobutene and Conversion into Surface Alkoxides, Angewandte Chemie-International Edition, 49 (2010) 4678-4680.
[27] C. Tuma, J. Sauer, Protonated isobutene in zeolites: tert-butyl cation or alkoxide?, Angewandte Chemie-International Edition, 44 (2005) 4769-4771.
[28] J.B. Nicholas, J.F. Haw, The prediction of persistent carbenium ions in zeolites, Journal of the American Chemical Society, 120 (1998) 11804-11805.
[29] H. Fang, A. Zheng, J. Xu, S. Li, Y. Chu, L. Chen, F. Deng, Theoretical Investigation of the Effects of the Zeolite Framework on the Stability of Carbenium Ions, J. Phys. Chem. C, 115 (2011) 7429-7439.
[30] H. Fang, A. Zheng, S. Li, J. Xu, L. Chen, F. Deng, New Insights into the Effects of Acid Strength on the Solid Acid-Catalyzed Reaction: Theoretical Calculation Study of Olefinic Hydrocarbon Protonation Reaction, J. Phys. Chem. C, 114 (2010) 10254-10264.
[31] W.L. Dai, C.M. Wang, X.F. Yi, A.M. Zheng, L.D. Li, G.J. Wu, N.J. Guan, Z.K. Xie, M. Dyballa, M. Hunger, Identification of tert-Butyl Cations in Zeolite H-ZSM-5: Evidence from NMR Spectroscopy and DFT Calculations, Angewandte Chemie-International Edition, 54 (2015) 8783-8786.
[32] J. Sauer, M. Sierka, Combining quantum mechanics and interatomic potential functions in ab initio studies of extended systems, Journal of Computational Chemistry, 21 (2000) 1470-1493.
[33] B.A. De Moor, M.F. Reyniers, G.B. Marin, Physisorption and chemisorption of alkanes and alkenes in H-FAU: a combined ab initio-statistical thermodynamics study, Physical Chemistry Chemical Physics, 11 (2009) 2939-2958.
[34] F. Goeltl, A. Grueneis, T. Bucko, J. Hafner, Van der Waals interactions between hydrocarbon molecules and zeolites: Periodic calculations at different levels of theory, from density functional theory to the random

phase approximation and Moller-Plesset perturbation theory, Journal of Chemical Physics, 137 (2012) 114111.
[35] F. Goeltl, J. Hafner, Modelling the adsorption of short alkanes in protonated chabazite: The impact of dispersion forces and temperature, Microporous Mesoporous Mat., 166 (2013) 176-184.
[36] J.Q. Chen, A. Bozzano, B. Glover, T. Fuglerud, S. Kvisle, Recent advancements in ethylene and propylene production using the UOP/Hydro MTO process, Catalysis Today, 106 (2005) 103-107.
[37] M.J. Tallman, C. Eng, Consider new catalytic routes for olefins production - Innovative catalyst systems enable higher propylene make from liquid feedstocks, Hydrocarbon Processing, 87 (2008) 95-+.
[38] T. von Aretin, S. Schallmoser, S. Standl, M. Tonigold, J.A. Lercher, O. Hinrichsen, Single-Event Kinetic Model for 1-Pentene Cracking on ZSM-5, Industrial & Engineering Chemistry Research, 54 (2015) 11792-11803.
[39] J. Abbot, B.W. Wojciechowski, THE MECHANISM OF CATALYTIC CRACKING OF NORMAL-ALKENES ON ZSM-5 ZEOLITE, Canadian Journal of Chemical Engineering, 63 (1985) 462-469.
[40] J.S. Buchanan, The chemistry of olefins production by ZSM-5 addition to catalytic cracking units, Catalysis Today, 55 (2000) 207-212.
[41] M.A. den Hollander, M. Wissink, M. Makkee, J.A. Moulijn, Gasoline conversion: reactivity towards cracking with equilibrated FCC and ZSM-5 catalysts, Appl. Catal. A-Gen., 223 (2002) 85-102.
[42] X.X. Zhu, S.L. Liu, Y.Q. Song, L.Y. Xu, Catalytic cracking of C4 alkenes to propene and ethene: Influences of zeolites pore structures and Si/Al-2 ratios, Appl. Catal. A-Gen., 288 (2005) 134-142.
[43] G. Kresse, J. Furthmuller, Efficient iterative schemes for ab initio total-energy calculations using a plane-wave basis set, Physical Review B, 54 (1996) 11169-11186.
[44] G. Kresse, J. Furthmüller, Efficiency of ab-initio total energy calculations for metals and semiconductors using a plane-wave basis set, Comput. Mat. Sci., 6 (1996) 15.
[45] G. Kresse, J. Hafner, ABINITIO MOLECULAR-DYNAMICS FOR LIQUID-METALS, Physical Review B, 47 (1993) 558-561.
[46] G. Kresse, J. Hafner, Ab initio molecular-dynamics simulation of the liquid-metal-amorphous-semiconductor transition in germanium, Phys. Rev. B, 49 (1994) 14251.
[47] T. Verstraelen, V. Van Speybroeck, M. Waroquier, ZEOBUILDER: A GUI toolkit for the construction of complex molecular structures on the nanoscale with building blocks, Journal of Chemical Information and Modeling, 48 (2008) 1530-1541.
[48] J. Van der Mynsbrugge, S.L.C. Moors, K. De Wispelaere, V. Van Speybroeck, Insight into the Formation and Reactivity of Framework-Bound Methoxide Species in H-ZSM-5 from Static and Dynamic Molecular Simulations, Chemcatchem, 6 (2014) 1906-1918.
[49] S. Grimme, J. Antony, S. Ehrlich, H. Krieg, A consistent and accurate ab initio parametrization of density functional dispersion correction (DFT-D) for the 94 elements H-Pu, Journal of Chemical Physics, 132 (2010) 154104.
[50] P.E. Blöchl, Projector augmented-wave method, Phys. Rev. B, 50 (1994) 17953.
[51] G. Kresse, D. Joubert, From ultrasoft pseudopotentials to the projector augmented-wave method, Physical Review B, 59 (1999) 1758-1775.
[52] S. Grimme, S. Ehrlich, L. Goerigk, Effect of the Damping Function in Dispersion Corrected Density Functional Theory, Journal of Computational Chemistry, 32 (2011) 1456-1465.
[53] M. Dion, H. Rydberg, E. Schroder, D.C. Langreth, B.I. Lundqvist, Van der Waals density functional for general geometries, Phys. Rev. Lett., 92 (2004) 246401.
[54] J. Wellendorff, K.T. Lundgaard, A. Mogelhoj, V. Petzold, D.D. Landis, J.K. Norskov, T. Bligaard, K.W. Jacobsen, Density functionals for surface science: Exchange-correlation model development with Bayesian error estimation, Physical Review B, 85 (2012) 235149.
[55] A. Ambrosetti, A.M. Reilly, R.A. DiStasio, Jr., A. Tkatchenko, Long-range correlation energy calculated from coupled atomic response functions, Journal of Chemical Physics, 140 (2014).
[56] T. Bučko, S. Lebègue, T. Gould, J. Ángyán, Many-body dispersion corrections for periodic systems: an efficient reciprocal space implementation, Journal of Physics: Condensed Matter, 28 (2016) 045201.

[57] A. Ghysels, T. Verstraelen, K. Hemelsoet, M. Waroquier, V. Van Speybroeck, TAMkin: A Versatile Package for Vibrational Analysis and Chemical Kinetics, Journal of Chemical Information and Modeling, 50 (2010) 1736-1750.
[58] J. VandeVondele, M. Krack, F. Mohamed, M. Parrinello, T. Chassaing, J. Hutter, QUICKSTEP: Fast and accurate density functional calculations using a mixed Gaussian and plane waves approach, Computer Physics Communications, 167 (2005) 103-128.
[59] G. Lippert, J. Hutter, M. Parrinello, The Gaussian and augmented-plane-wave density functional method for ab initio molecular dynamics simulations, Theoretical Chemistry Accounts, 103 (1999) 124-140.
[60] G. Lippert, J. Hutter, M. Parrinello, A hybrid Gaussian and plane wave density functional scheme, Molecular Physics, 92 (1997) 477-487.
[61] K. Yang, J.J. Zheng, Y. Zhao, D.G. Truhlar, Tests of the RPBE, revPBE, tau-HCTHhyb, omega B97X-D, and MOHLYP density functional approximations and 29 others against representative databases for diverse bond energies and barrier heights in catalysis, Journal of Chemical Physics, 132 (2010) 10.
[62] S. Goedecker, M. Teter, J. Hutter, Separable dual-space Gaussian pseudopotentials, Physical Review B, 54 (1996) 1703-1710.
[63] K. De Wispelaere, B. Ensing, A. Ghysels, E.J. Meijer, V. Van Speybroeck, Complex Reaction Environments and Competing Reaction Mechanisms in Zeolite Catalysis: Insights from Advanced Molecular Dynamics, Chem.-Eur. J., 21 (2015) 9385-9396.
[64] S.L.C. Moors, K. De Wispelaere, J. Van der Mynsbrugge, M. Waroquier, V. Van Speybroeck, Molecular Dynamics Kinetic Study on the Zeolite-Catalyzed Benzene Methylation in ZSM-5, Acs Catalysis, 3 (2013) 2556-2567.
[65] F. Goltl, J. Hafner, Alkane adsorption in Na-exchanged chabazite: The influence of dispersion forces, Journal of Chemical Physics, 134 (2011) 064102.
[66] L. Schimka, J. Harl, A. Stroppa, A. Grueneis, M. Marsman, F. Mittendorfer, G. Kresse, Accurate surface and adsorption energies from many-body perturbation theory, Nat. Mater., 9 (2010) 741-744.
[67] D. Frenkel, B. Smit, Understanding Molecular Simulation, Academic Press, Inc., 2001.
[68] A. Laio, F.L. Gervasio, Metadynamics: a method to simulate rare events and reconstruct the free energy in biophysics, chemistry and material science, Rep. Prog. Phys., 71 (2008) 126601.
[69] A. Laio, M. Parrinello, Escaping free-energy minima, Proceedings of the National Academy of Sciences of the United States of America, 99 (2002) 12562-12566.
[70] K. De Wispelaere, S. Bailleul, V. Van Speybroeck, Catal. Sci. Technol., (2016).
[71] B. Ensing, A. Laio, M. Parrinello, M.L. Klein, A recipe for the computation of the free energy barrier and the lowest free energy path of concerted reactions, Journal of Physical Chemistry B, 109 (2005) 6676-6687.
[72] F. Goeltl, P. Sautet, Modeling the adsorption of short alkanes in the zeolite SSZ-13 using "van der Waals" DFT exchange correlation functionals: Understanding the advantages and limitations of such functionals, Journal of Chemical Physics, 140 (2014) 154105.
[73] C.-C. Chiu, G.N. Vayssilov, A. Genest, A. Borgna, N. Roesch, Predicting Adsorption Enthalpies on Silicalite and HZSM-5: A Benchmark Study on DFT Strategies Addressing Dispersion Interactions, Journal of Computational Chemistry, 35 (2014) 809-819.

*Manuscript
Click here to view linked References

On the stability and nature of adsorbed pentene in Brønsted acid zeolite H-ZSM-5 at 323 K

*J. Hajek , J. Van der Mynsbrugge, K. De Wispelaere , P. Cnudde, L. Vanduyfhuys, M. Waroquier and V. Van Speybroeck**

Center for Molecular Modeling, Ghent University, Technologiepark 903, B-9052 Zwijnaarde, Belgium

*Corresponding author:

veronique.vanspeybroeck@ugent.be

ABSTRACT: Adsorption of linear pentenes in H-ZSM-5 at 323 K is investigated using contemporary static and molecular dynamics methods. A physisorbed complex corresponding to free pentene, a π-complex and a chemisorbed species may occur. The chemisorbed species can either be a covalently bonded alkoxide or an ion pair, a so-called carbenium ion. Without finite temperature effects, the π-complex is systematically slightly more bound than the chemisorbed alkoxide complex, whereas molecular dynamics calculations at 323 K yield an almost equal stability of both species. The carbenium ion was not observed during simulations at 323 K. The transformation from the π-complex to the chemisorbed complex is activated by a free energy in the range of 33-42 kJ/mol. Our observations yield unprecedented insights into the stability of elusive intermediates in zeolite catalysis, for which experimental data are very hard to measure.

1. Introduction

Solid acids such as zeolites are widely applied in the chemical industry for conversion of hydrocarbons in reactions such as catalytic cracking, hydrocracking and alkylation.[1-6] These reactions involve alkanes and alkenes as reactants and products which interact with the zeolite and its Brønsted acid sites (BAS).[7] The understanding of alkane adsorption on various zeolites has been the subject of numerous experimental studies, whereas comparatively little is known about adsorption of alkenes, due to their high reactivity even at low temperatures. [8-10]

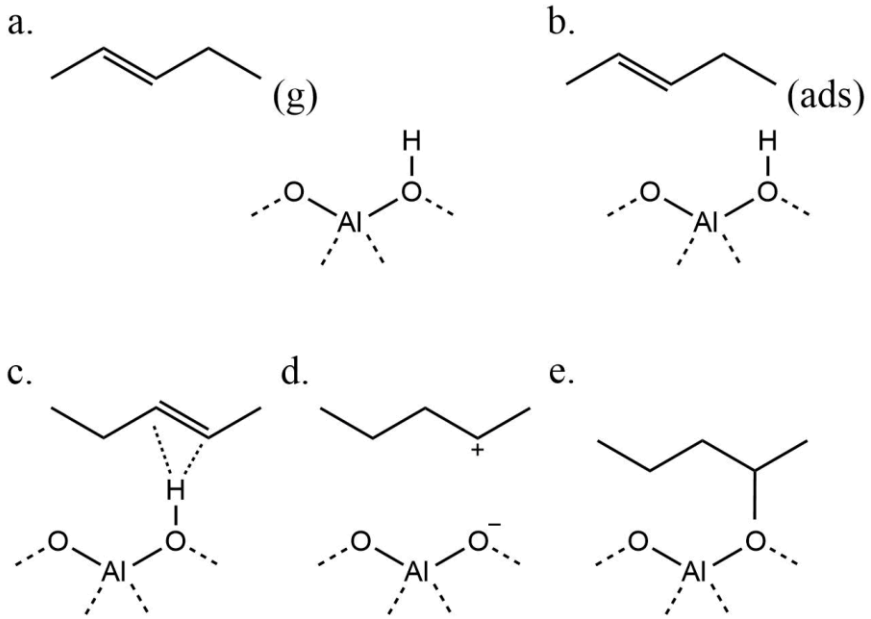

Figure 1: Illustration of the different intermediates upon alkene (2-pentene) adsorption in the presence of a Brønsted acid site (BAS): (a) alkene in gas phase, (b) alkene physisorbed in the channels of the zeolite (c) alkene π-complex, (d) chemisorbed carbenium ion (e) chemisorbed alkoxide.

When an alkene adsorbs on a Brønsted acid zeolite, various adsorbed species may be distinguished as schematically indicated in Figure 1. [11-14] A first state corresponds to a free alkene in the cages of the zeolite, which undergoes only a weak van der Waals (vdW) interaction with the walls of the zeolite. This state is further referred to as the physisorbed state. A more bound state corresponds to the π-complex, where a specific non-bonded interaction between the π-electrons of the double bond and the Brønsted acid site occurs. Finally the π-complex may be protonated leading to the formation of a chemisorbed species. [11-14] The nature of the resulting intermediate is still debated. It has been proposed to be stabilized as a covalently bonded alkoxide or as an ion pair which is referred to as a free carbenium ion (Figure 1). [11, 12, 15-17]

Alkene adsorption is very difficult to track experimentally as these hydrocarbons are highly reactive even at low temperatures. Solely based on experiment it is practically excluded to gain insight into the nature of the adsorbed complexes and intermediates, which can be very short-lived. For butenes some NMR and infrared based adsorption studies are available. The adsorption of butenes on H-ZSM-5 and mordenite was experimentally investigated by Domen et al. [12, 13, 17-19] On H-ZSM-5, they observed that at sub-ambient temperatures a stable π-complex was formed and that double bond isomerization occurred already at 230 K. [13, 18, 20] A concerted mechanism was suggested to explain the rapid double bond isomerization despite the absence of a classical carbenium ion at these temperatures, as evidenced from isotope experiments.[20-22] Isotope experiments evidenced in addition the high mobility of alkenes already at sub-ambient

temperatures. [18, 20] Stepanov et al. studied the kinetics of the double-bond shift reaction, H/D exchange and ^{13}C scrambling for linear butenes on FER by means of ^{1}H, ^{2}H and ^{13}C MAS NMR for temperatures above 290 K and determined activation energies for the double bond shift and showed that carbenium ions are involved in the mechanism of double bond isomerization at higher temperatures. [21, 23]

Due to the lack of experimental data, theoretical studies are indispensable to obtain insight into the nature and stability of adsorbed species. Adsorption of alkanes has been studied extensively in literature by various theoretical methods. A more complete literature overview may be found in some recent reviews. [24, 25] For alkenes much less information is available also from a theoretical point of view. In a series of papers by Sauer and co-workers various theoretical methods were used to study the adsorption behavior of C4 species in H-FER. [26, 27] The methods varied in the treatment of the molecular environment, the method to account for the long range dispersion interactions and the degree to which finite temperature effects were accounted for. All three factors are decisive to determine the relative stabilities of the π-complex, carbenium ions and alkoxide species. The stability of carbenium ions not only depends on the carbon skeleton, i.e. secondary, tertiary, cyclic, but also largely on the applied temperature. Higher temperatures may favor the existence of persistent carbenium ions. Nicholas and Haw concluded that stable carbenium ions could be observed by NMR provided that the neutral compound from which it originates has a proton affinity of 875 kJ mol^{-1} or larger.[28] However the topology of the material may also be very important as was shown by Fang et al. [29, 30] It was only very recently that the tert-butyl cation on H-ZSM-5 was identified by capturing this reaction intermediate with an ammonia molecule and by identifying the stable surface compounds by $^{1}H/^{13}C$ magic angle spinning NMR spectroscopy and density functional theory calculations. [31] The physisorption and chemisorption of alkenes beyond C4 in a variety of zeolites (H-FAU, H-BEA, H-MOR, H-ZSM-5) was studied by Marin and co-workers using the QM-Pot methodology originally developed by Sauer and co-workers. [14, 32, 33] The method relies on a combination of a quantum mechanics approach on a smaller part of the system combined with an interatomic potential approach on the periodic structure. The QM-Pot methodology has proven very valuable in the time frame where periodic static calculations with more advanced functionals and dispersion interactions were unfeasible. Some earlier theoretical works also reported on the relative stabilities of alkenes, but this was done in absence of dispersion interactions, however also the importance of various rotational orientations of the adsorbed species was emphasized. [11] Indeed Göltl and co-workers stressed the role of finite temperature effects and mobility of adsorbed species in case of alkanes. For methane, ethane and propane in protonated chabazite at 300 K there was a substantial probability that the adsorbate desorbs from the acid site and moves freely in the pores of the zeolite, yielding adsorption enthalpies which are systematically smaller than the prediction at 0 K. [34, 35]

To the best of our knowledge no experimental data are available for alkene adsorption in H-ZSM-5 beyond C4. Furthermore no fully periodic density functional theory calculations are available for the various adsorbed species of alkenes higher than C4, neither from static calculations at 0 K nor from molecular dynamics calculations to account for finite temperature effects on the adsorption behavior. Such understanding is however crucial to optimize industrially important processes such as olefin cracking. These processes receive a lot of interest to selectively produce propene, by cracking less valuable C_4 through C_8 olefins. [36-38] Alkene cracking processes consist of a complex reaction network including isomerizations, oligomerizations, alkylations, hydride transfers and cracking reactions. [3, 7, 39] In any case, knowledge on the reaction intermediates is of utmost importance.

In this paper we present a complete study on the adsorption behavior of linear pentenes in H-ZSM-5, which is one of the most effective industrial catalysts in light olefin production due to its optimal balance between conversion, selectivity and coke formation stability. [40-42] The applied methodology encompasses static periodic density functional theory calculations using contemporary density functionals and methods to account for the dispersion interactions, first principle molecular dynamics simulations at 323 K to account for the mobility of the adsorbates, and metadynamics simulations to sample the transformations among π-complex, alkoxide and carbenium ion and to deduce the corresponding free energy barriers. This complementary set of tools provides an overall picture of the various adsorbed species in the absence of current relevant experimental data. Such insights into the relative stability of adsorbed species is of fundamental importance for our understanding of zeolite catalysis.

2. Computational Methods

H-ZSM-5 was represented by a periodic model to fully account for the zeolitic surroundings (Figure S.1 of the SI). Static periodic Density Functional Theory (DFT) calculations were performed with the Vienna Ab Initio Simulation Package (VASP 5.3). [43-46] Initial geometries were constructed with ZEOBUILDER. [47] The position of the Brønsted acid site (BAS) is the same as in earlier works of the authors [24, 48] with a substitutional aluminum at the T12 position of the orthorhombic MFI unit cell and the charge compensating proton on O_{20} , resulting in a BAS at the intersection of the straight and sinusoidal channels (Figure S.1). All structures were first optimized with a PBE functional using Grimme D3 dispersion corrections. [49] During the calculations the projector augmented approximation (PAW) [50, 51] together with a plane wave kinetic energy cutoff of 600 eV were used and sampling of the Brillouin zone was restricted to the Γ-point. The convergence criterion for the electronic self-consistent field (SCF) problem was set to 10^{-5} eV. For all static

periodic DFT calculations the unit cell was relaxed during the geometry optimizations. Afterward, the energy was refined with a variety of exchange correlation functionals and dispersion models encompassing revPBE-D3 with and without Becke Johnson damping (BJ) [52], revPBE with the non-local correlation functional vdW-DF of Dion [53], BEEF-vdW [54], and PBE with the new many body dispersion (MBD) scheme of Tkatchenko with conventional (MBD-vdW_H) and iterative Hirshfeld partitioning (MBD-vdW_HI). [55, 56] The thermal corrections were performed on the basis of frequencies obtained with a partial Hessian approach including 8T atoms, the acid proton and the adsorbate. De Moor et al. [8] demonstrated that this type of procedure of using a partial Hessian is sufficient to determine accurate enthalpy and entropy differences. The nature of the local minima was verified by a normal mode analysis and the obtained partial Hessian matrix included only positive eigenmodes. We applied the partial Hessian vibrational analysis (PHVA) [55–57] as implemented in an in-house post-processing toolkit TAMkin. [57]

Ab initio molecular dynamics (MD) simulations were performed with the CP2K software package [58] on the DFT level of theory by using the combined Gaussian Plane Wave basis sets approach. [59, 60] The revPBE-D3 functional [61] together with the DZVP-GTH basis set and pseudopotentials were chosen. [62] This combination of exchange correlation functional and dispersion model was successfully used in earlier zeolite catalysis work. [48, 63, 64] Since ab initio molecular dynamics calculations performed on the complete zeolite model are computationally very expensive, more advanced methods using hybrid functionals or many body dispersion models are not feasible for simulations of considerable time length as emphasized here. [65, 66] The cell parameters were determined from a preliminary NPT run on the empty zeolite unit cell at 323K and 1 atm and are found to be a = 20.14 Å, b = 20.33 Å, c = 13.56 Å, α = 89.82 °, β = 89.47 °, γ = 90.15°. Subsequent molecular dynamics and metadynamics (cf. infra) simulations on the various complexes were performed in the NVT ensemble at 323K. The integration time step was set to 0.5 fs. The temperature was controlled by a chain of five Nosé-Hoover thermostats. [67] The MD simulations also allow the computation of finite-temperature adsorption enthalpies for the various π-complexes and alkoxides from ensemble averages of the internal energies over the MD trajectories from separate simulations on the complex, the empty zeolite and the adsorbate in gas phase. More details on the procedure and the influence of the length of the MD runs are given in the SI.

To accelerate sampling of the activated transition from the π-complex to the pentoxide and to explore the nature of the carbenium ion, a metadynamics (MTD) approach was employed. [68, 69] This method has recently been applied successfully in various zeolite catalysis studies. [63, 70] During an NVT MTD run with similar settings as for the MD simulations, Gaussian hills are added every 25 fs along two collective variables (CVs), described by coordination numbers (CN), which are able to describe the reaction coordinate for

transformations between the various adsorbed species. The first CV is defined by CN(H-O) – CN(H-C1) and describes the proton transfer from the zeolite to the pentene; the second CV is defined by CN(C2-Oz) and describes the formation of the C-O bond between the resulting pentyl carbenium ion and the zeolite framework. C1 and C2 are the carbon atoms forming the double bond and visualized in **Figure 2** together with the definition of the collective variables. The metadynamics simulations yield a two-dimensional free energy surface in terms of the two collective variables. A 1D free energy profile is constructed by projecting the 2D free energy onto the minimum free energy path after which the free energy of activation may be computed. [71] More technical details of the simulations are taken up in the SI.

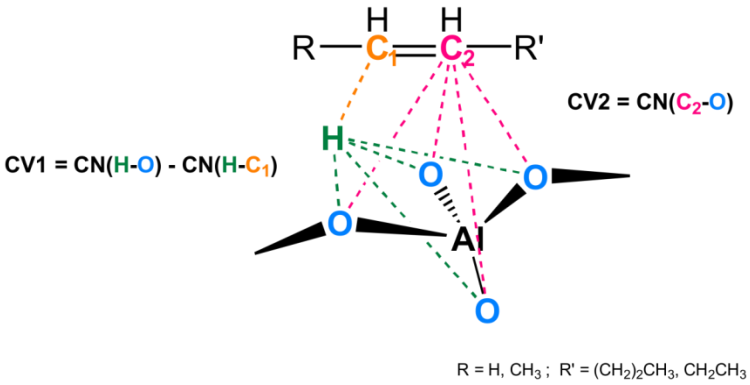

Figure 2: Schematic visualization of the collective variables used for the various metadynamics simulations.

3. Results and discussion

To obtain insight into the mobility of the various adsorbed pentene species and the various plausible configurations, a series of ab initio MD runs were performed at 323 K on 1-pentene (π), 2-pentene (π), 2-pentoxide and 3-pentoxide complexes. As the potential energy surface (PES) contains a large number of local minima, we first performed a number of short MD runs of about 10 ps starting from an unbiased initial position corresponding to an orientation of the physisorbed pentene molecule in the center of the straight 10-membered ring cavity at about 4 Å from the acid site. We followed how the 2-pentene evolved during the initial stages of the simulation. In the Supporting Information we display some snapshots. The adsorbate which only interacts with the walls of the zeolite, quickly diffuses towards the acid site to form the π-complex. The 2-pentene molecule is preferentially positioned with the methyl end directed in the sinusoidal channel near the BAS and the longer ethyl tail in the straight cavity. These initial MD runs are then followed by more extensive production molecular dynamics runs of 100 ps starting from the optimal configuration obtained from the initial MD runs. The π-complex is characterized by the distance between the C=C double

bond and the acid proton (H_z). The probability distribution of the shortest distance between one of the carbon atoms in the double bond and the acid proton during the simulation is plotted in **Figure 3**. For both 1- and 2-pentene the shortest C-H_z distance is on average about 2 Å, indicating that the π-H interaction remains in place throughout the simulation. During the simulations at 323 K we did not observe the carbenium ion. For the alkoxides a similar analysis was done, yielding average C-O_z distances of about 1.6 Å, indicating that these complexes also remain stable during the simulation.

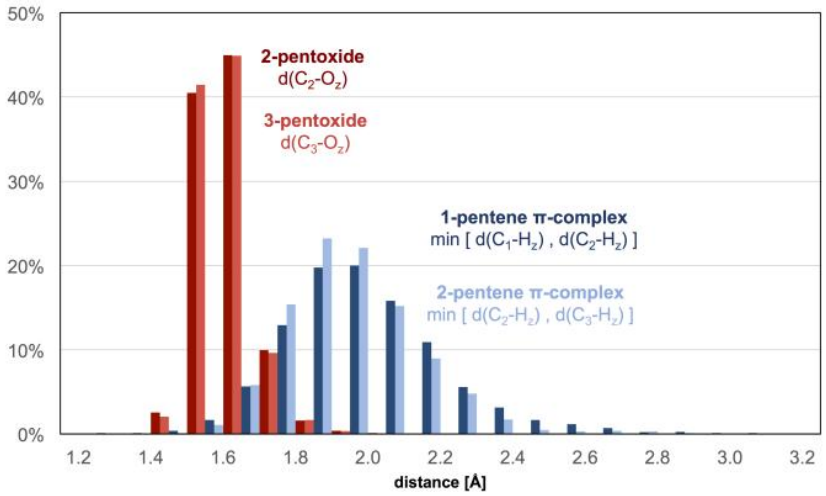

Figure 3: Probability distributions of some critical distances in molecular dynamics simulations of π-complexes and alkoxides in H-ZSM-5 obtained over a 60 ps run. Min[d(C_1-H_z),d(C_2-H_z)] stands for the shortest C-H_z distance in 1-pentene π-complex [average 2.07 Å]; Min[d(C_2-H_z),d(C_3-H_z)] stands for the shortest distance in the 2-pentene π-complex [average : 2.04 Å]; d(C_2-O_z) is the C_2-O_z distance in 2-pentoxide complex [average: 1.62 Å]; and d(C_3-O_z) is the C_3-O_z distance in 3-pentoxide complex [average: 1.62 Å].

Besides geometrical features MD simulations also release information about adsorption enthalpies. They are discussed further in the text where we investigated the influence of finite temperature effects on the adsorption process. First we report the 0 K results predicted by static calculations for the most visited structures.

In a next step, based on the probability distribution (Figure 3) we determined adsorption positions corresponding to the most frequently visited structures during the MD runs and performed static calculations on these initial structures to get the optimized geometries. Subsequent frequency calculations lead finally to the adsorption enthalpies. For 1- and 2-pentene the energetically favorable configuration corresponds to the

adsorbate positioned in straight channel with its methyl tail oriented into the zigzag channel. The most plausible structures are visualized in Figure 4. To ensure that the selected geometries for the static calculations do not substantially influence the obtained energetics, additional geometry optimizations were performed on a range of other geometries also generated from MD simulations. More details are taken up in Section 3.1 of the SI.

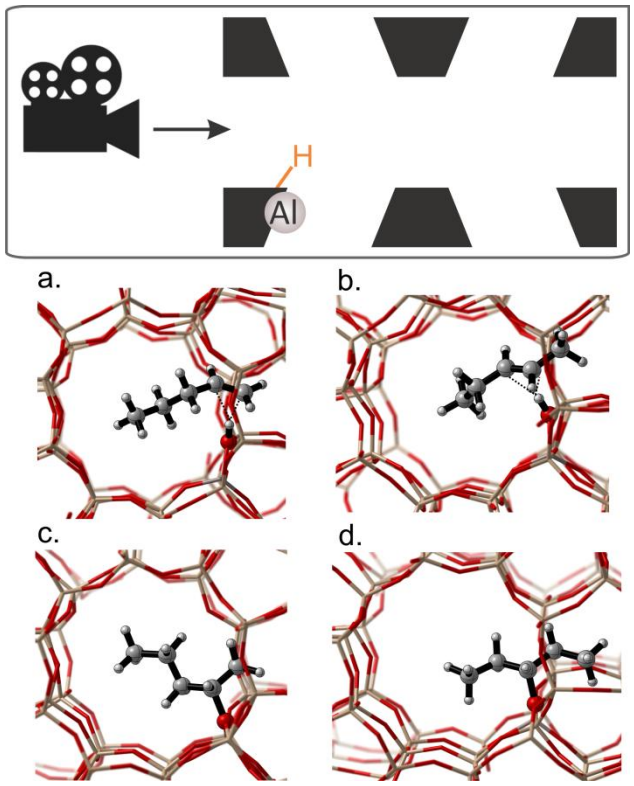

Figure 4: MD snapshots of a) 1-pentene π-complex, b) 2-pentene π-complex, c) chemisorbed 2-alkoxide, d) chemisorbed 3-alkoxide in H-ZSM-5 at 323K, seen in the direction of the straight channel (camera viewpoint). The snapshots correspond to geometries which are most frequently visited during MD runs of 100 ps at 323 K.

A decisive parameter for the energetics of the adsorbed species is the distance of the carbon skeleton with respect to the BAS. After optimization, the 1-pentene π-complex has a characteristic shortest C-H_z distance of about 1.9 Å. For 2-pentene π-complex this is about 2 Å. The pentoxide species are characterized by a C-O_z distance of about 1.6 Å . In order to check the influence of different functionals and dispersion models, we refined the energies using revPBE [53] and BEEF [54] functionals. Also some recently introduced dispersion models were tested such as the models of Tkatchenko et al. [55, 56] An overview of the adsorption enthalpies and free energies is given in Table S.3 of the SI. All applied level of theories (LOT's) systematically predict the π-complexes more stable with respect to their chemisorbed counterparts by some

15-30 kJ/mol. The qualitative trends remain the same for all used levels of theory. The results show that the Becke-Johnson (BJ) damping function [52], revPBE-vdW-DF and BEEF-vdW levels of theory, even substantially enlarge the stability of the π-complexes compared with all other dispersion models, which indicates that these methods predict an overbinding of the adsorbed species.

Table 1: Free energy ΔG and enthalpy ΔH differences for configurations for the π-complex and chemisorbed complex in H-ZSM-5 at 323 K. All energies in kJ/mol. Use of the standard notation "LOT-E"//"LOT-G" (LOT-E and LOT-G being the electronic levels of theory used for the energy and geometry optimizations, respectively).

	PBE-D3 //PBE- D3		revPBE-D3 //PBE- D3		revPBE-D3(BJ) //PBE D3		revPBE-vdW-DF //PBE D3		BEEF-vDW //PBE D3		PBE-MBD-vdW_H//PBE D3		PBE-MBD-vdW_HI//PBE D3	
	ΔG	**ΔH**	**ΔG**	**ΔH**	**ΔG**	**ΔH**	**ΔG**	**ΔH**	**ΔG**	**ΔH**	**ΔG**	**ΔH**	**ΔG**	**ΔH**
1-pentene (g) -> 1-pentene (π)	-45.0	-103.2	-58.4	-116.6	-76.1	-134.3	-106.7	-164.9	-68.4	-126.6	-51.3	-109.5	-39.9	-98.1
2-pentene (g) -> 2-pentene (π)	-52.7	-109.6	-73.3	-130.2	-90.7	-147.6	-112.4	-169.2	-71.1	-128.0	-58.6	-115.5	-44.7	-101.6
1-pentene (g) -> 2-pentoxide	-17.5	-84.9	-40.1	-107.5	-60.3	-127.8	-69.2	-136.6	-29.4	-96.8	-30.6	-98.0	-15.0	-82.5
2-pentene (g) -> 2-pentoxide	-4.1	-72.2	-28.7	-96.8	-47.4	-115.6	-58.2	-126.4	-17.8	-86.0	-17.2	-85.3	-1.4	-69.6
2-pentene (g) -> 3-pentoxide	-3.0	-68.8	-21.3	-87.1	-39.8	-105.6	-52.9	-118.7	-14.1	-80.0	-19.9	-85.7	-2.8	-68.6
1-pentene (π) -> 2-pentoxide	27.5	18.3	18.3	9.1	15.8	6.6	37.6	28.3	39.0	29.8	20.7	11.5	24.9	15.7
2-pentene (π) -> 2-pentoxide	48.6	37.4	44.6	33.3	43.3	32.0	54.1	42.8	53.3	42.0	41.4	30.1	43.3	32.0
2-pentene (π) -> 3-pentoxide	49.7	40.8	52.0	43.0	50.9	42.0	59.5	50.5	57.0	48.0	38.7	29.8	41.9	33.0

Göltl and co-workers reached similar conclusions for the revPBE-vdW-DF method and an in depth analysis was presented more recently by Göltl and Sautet. [72]

To investigate also the influence of the level of theory on the geometry optimization and the derived relative stabilities of the π-complex and alkoxide structures, we also performed new geometry optimizations and frequency calculations for 2-pentene π- complex and 2-pentoxide using the BEEF-vdW functional [54]. Geometrical details of the structures with PBE-D3 and BEEF-vdW functionals are given in **Table S.4**. There are no essential features which are different, but the most crucial result is that the free energy and the adsorption enthalpy differences for the π-complex and chemisorbed complex are very similar to each other (see **Table 2**) confirming our conclusions for the static calculations.

Table 2 : Free energy ΔG and enthalpy ΔH differences for configurations for the π-complex and chemisorbed complex in H-ZSM-5 at 323 K given in kJ/mol.

	BEEF-vdW //PBE D3		BEEF-vdW // BEEF-vdW	
	ΔG	**ΔH**	**ΔG**	**ΔH**
2-pentene (π) -> 2-pentoxide	53.27	41.96	51.05	42.7

Our theoretical findings give qualitatively and quantitatively different results than the values of Nguyen et al. produced with the QM-Pot methodology. [14] Recently, also Rosch et al. found similar deviating behavior for alkanes between periodic DFT and QM-Pot results. [73] A proper analysis of possible ingredients lying on the origin of the observed differences, learns that the deviancies should not be ascribed to the QM-Pot methodology itself, but mainly to less favorite geometries of the adsorbed species and their positions in the cavity. In the case studied by Nguyen et al. [14], the double bond of 1- and 2-pentene was located at about 2.3 Å from the BAS, which is significantly larger than the distances predicted in this work. The PES around the adsorption site was explored in a 4T cluster embedded in the zeolite unit cell, and is by far not as accurate as the present calculations where the influence of the environment on the PES is intensively investigated in first-principles MD simulations of the periodic models. The geometries for 1- and 2-pentene reported in ref. [14] differ by far from the configurations obtained in this work. On the other hand the geometrical parameters of the corresponding pentoxides found in the two studies are completely similar, so that the difference in stability between the physisorbed and chemisorbed complexes must be ascribed to the position of the physisorbed pentene to the BAS. This is an important statement as it reduces the discussion on the

exothermic or endothermic character of the chemisorption process to the localization of the adsorbed pentene π-complex in the pores of the zeolite and more particularly the distance from the BAS.

In a next step, we assessed the influence of finite temperature effects on the adsorption enthalpies. The probability distributions for the distances of the various adsorbed species to the BAS, reveal an asymmetric behavior for the π-complexes towards higher C-H distances. For 1-pentene this is even more pronounced than for 2-pentene. The adsorption enthalpy of 1- and 2- pentene is strongly correlated with the C-H distance. The broad probability distribution for these two species clearly indicates that the average ensemble over the MD trajectories results in enthalpy of adsorption which corresponds to larger C-H distances than 2 Å. On the other hand, the static calculations only consider one point on the potential energy surface (that corresponds to the optimized geometry) and do not account for configurations with slightly larger distances as observed in the MD simulations. Indeed the dynamically averaged values for the adsorption enthalpies yield systematically lower adsorption enthalpies for the π-complexes and slightly larger values for the alkoxides. The adsorption enthalpies for the π-complexes are shifted with about 20 kJ/mol. **Figure 3** also reveals that the C-O_z distances in the pentoxides are more peaked around 1.6 Å with almost 80 % probability yielding slightly more bound adsorption enthalpies from MD simulations. The adsorption enthalpies of pentoxides obtained as an ensemble average in the MD simulations are closer to the values obtained with static approaches. If finite temperature effects are taken into account the π-complexes are almost equally stable as the alkoxide species. A summarizing adsorption enthalpy diagram is given in **Figure 5**. In good agreement with ref [11], the double bond position does not affect significantly the enthalpy of formation of the π-complex. Static calculations systematically overestimate the adsorption enthalpies for the π-complex, which is inherently related to the usage of optimized geometries, which are necessary to compute enthalpic and entropic contributions, but neglect the asymmetric probability distribution shown in **Figure 3** at finite temperatures.

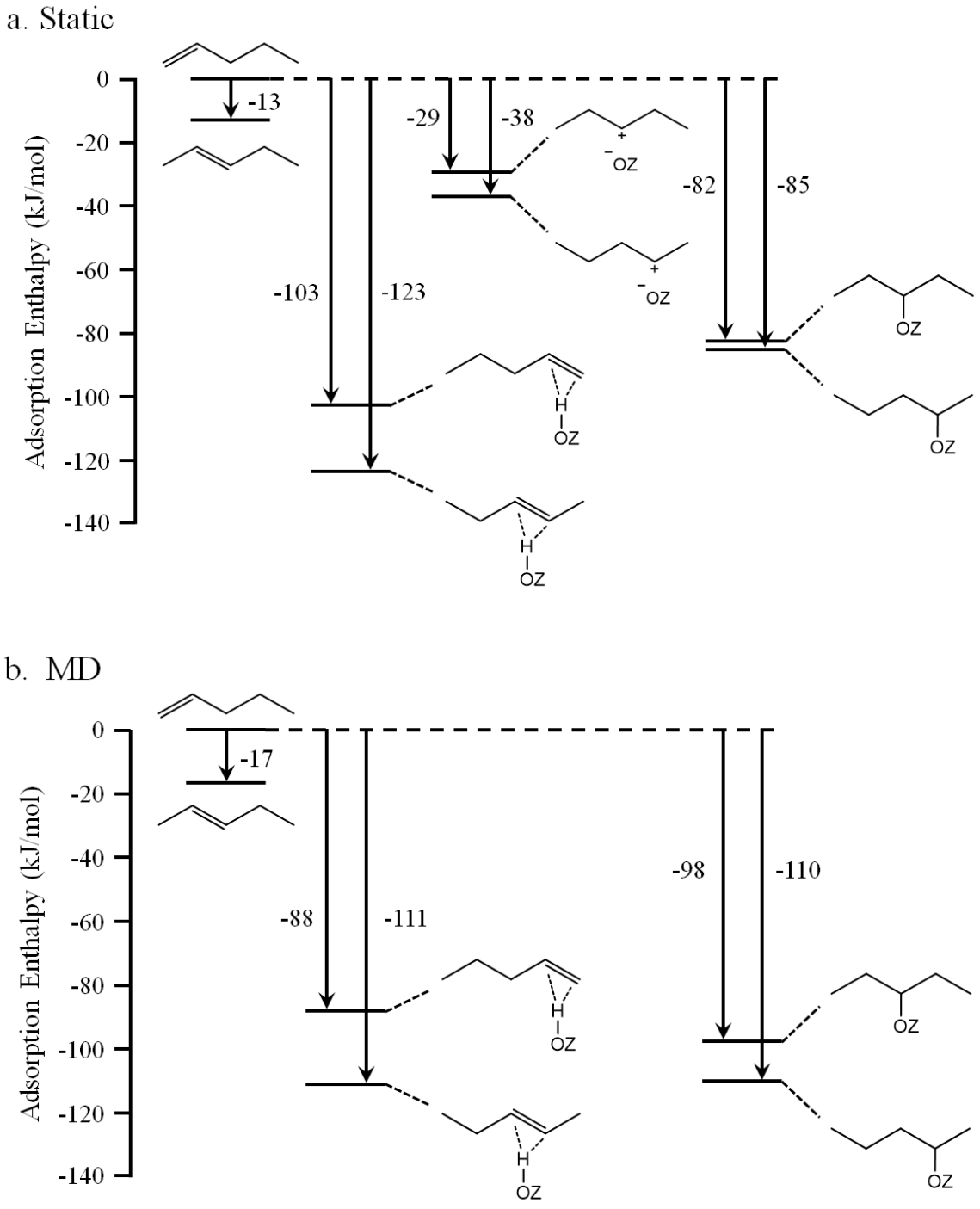

Figure 5. Adsorption enthalpy diagrams at 323 K for the several pentene intermediates with reference to 1-pentene in gas phase and an empty H-ZSM-5 framework, obtained from (a) static calculations at the PBE-D3 level (b) MD simulations at the revPBE-D3 level.

Finally we also wanted to investigate the possible occurrence of carbenium ions in the transition path from π-complexes to alkoxides. Therefore we used metadynamics simulations which allowed to sample the transition from the π-complex towards the chemisorbed species and to explore in how far the transformation is activated. Those simulations allow yielding detailed information on the nature of the chemisorbed species and the possible existence of a carbenium ion. In any case the carbenium ion was not observed during a regular MD run, nor was the transition from the π-complex towards the alkoxide seen, which points towards an activated transition.

The formation of 2-pentoxide from physisorbed 1-pentene and 2-pentene and that of 3-pentoxide from physisorbed 2-pentene were studied using metadynamics simulations with two collective variables to describe the reaction coordinate (cfr. Computational Methods). The resulting 2D free energy surfaces and 1D free energy profiles along the lowest free energy paths corresponding with the three reactions are displayed in **Figure 6**. There clearly exists a metastable state between the pentene π-complex and the pentoxide, which could be characterized as a carbenium ion. This metastable state mainly represents a 2-pentyl carbenium ion in the two reactions leading to 2-pentoxide; however, rapid isomerization to a 3-pentyl carbenium ion was observed as well.

In a next step the trajectories obtained from the metadynamics simulations were examined to distinguish between the free energy minima of the various adsorbed species. All samples in which the collective variable, corresponding to the coordination number representative for the C-O_z bond formation with the zeolite framework, is smaller than a cutoff value are identified as alkoxides. A similar procedure was applied for the identification of the pentyl carbenium ions. The detailed procedure is described in the SI. The procedure shows that it is possible to identify various basins corresponding to alkoxides where the C-O distance is on average 1.6 Å and corresponding to carbenium ions where the average distance is 3 Å, which is significantly larger than the value (2.0 Å) obtained with MD simulations for the π-complex (**Figure 3**). Here, some prudence should be taken into consideration as metadynamics does not generate an equilibrium ensemble and hence geometric parameters, given in MTD, are only indicative.

The 2D free energy surface is subsequently converted into a 1D free energy profile (by projection onto the minimum free energy path). For the three reactions under study the difference (CV2-CV1) of the two coordinations numbers turned out to be a good estimate for the one-dimensional reaction coordinate. The three free energy profiles for pentoxide formation, displayed in Figure 6, show the carbenium ion as a metastable intermediate between the π-complex and the alkoxide. They also allow to determine the free energy barriers ($\Delta G^{\ddagger}$) and reaction free energies (ΔG_r) between the various intermediate states following a procedure outlined in the SI. They are listed in Table 3.

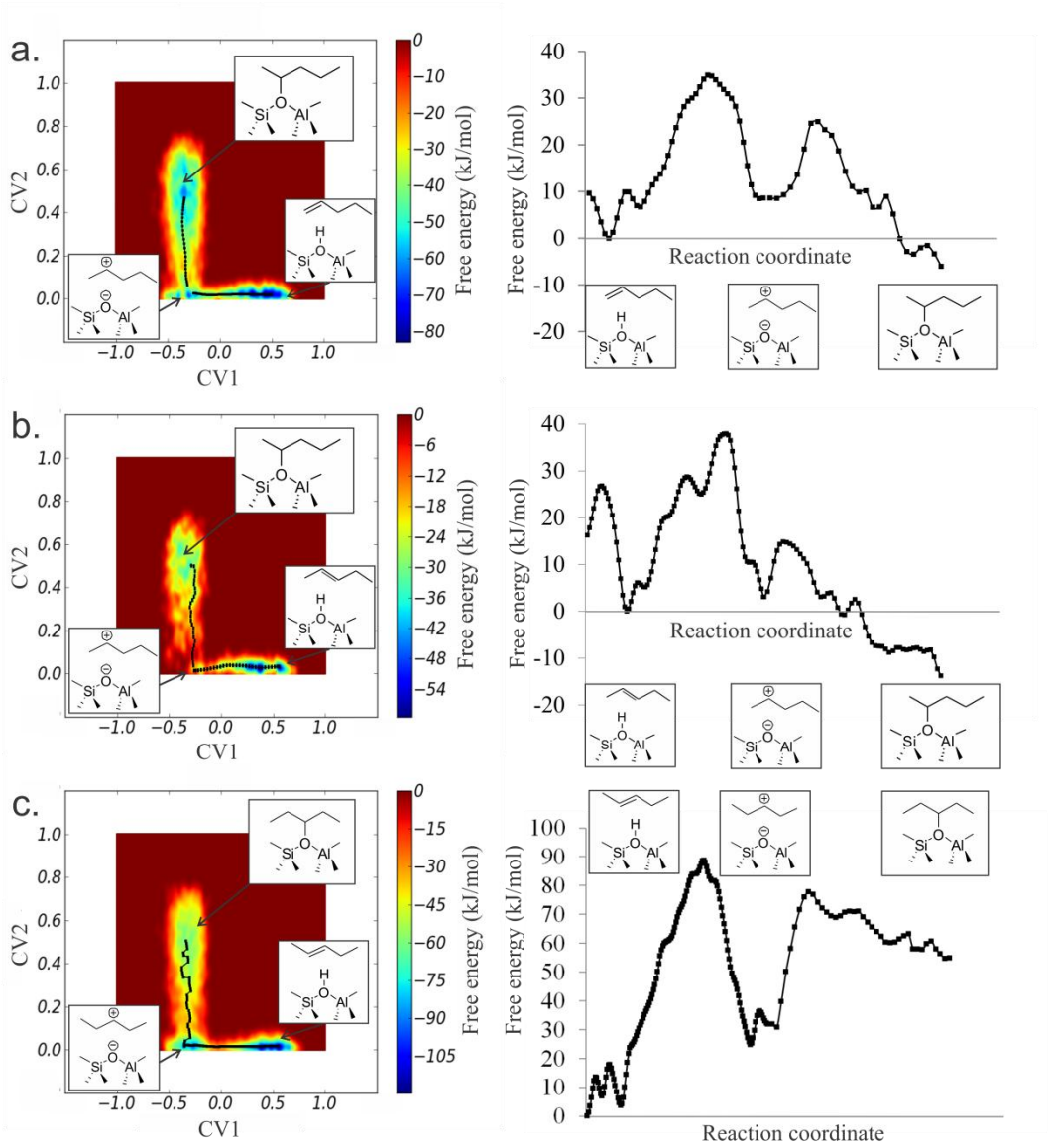

Figure 6. Left: 2D free energy surface for the formation of 2-pentoxide from a 1-pentene π-complex (a) or 2-pentene π-complex (b) and for the formation of 3-pentoxide from a 2-pentene π-complex (c) . The lowest free energy paths are displayed. A small well corresponding to the metastable carbenium ion can be observed in the bottom left corner. Right: corresponding 1D free energy profile along the lowest free energy path for the two reactions.

Table 3. Free energy barriers ($\Delta G^{\ddagger}$) and reaction free energies (ΔG_r) in kJ/mol at 323 K for the formation of a pentoxide from a pentene π-complex through a carbenium ion intermediate determined from MTD simulation in the NVT ensemble. LOT electronic energies: revPBE-D3/DZVP-GTH.

	$\Delta G^{\ddagger}$ (323 K) [kJ/mol]	**ΔG_r (323 K) [kJ/mol]**
1-pentene (π) → 2-pentyl carbenium	36.8	-2.3
2-pentyl carbenium → 2-pentoxide	20.3	-9.2
2-pentene (π) → 2-pentyl carbenium	38.2	+2.8
2-pentyl carbenium → 2-pentoxide	12.1	-15.2
2-pentene (π) -> 3-pentyl carbenium	84.7	+22.9
3-pentyl carbenium -> 3-pentoxide	54.6	+34.3

The observed free energy barriers for activation between the π-complex and the chemisorbed species largely vary from the type of the chemisorption process. The formation of 2-pentoxides is likely to occur at these temperatures as the free energy of activation corresponds to about 36.8 kJ/mol for 1-pentene to 2-pentyl carbenium ion and 38.2 kJ/mol for 2-pentene to 2-pentyl carbenium ion. The formation of 3-pentoxide is less probable, a higher free energy of activation is found and the formed 3-pentoxide is less stable than the other alkoxides. This observation is systematically found for all methodologies used in this work, and is probably due to unfavorable steric interactions with the walls of the zeolite. MD simulations have revealed that by preference the shortest tail of the chemisorbed pentoxide is oriented in the zigzag channel. For a 2-pentoxide it is a methyl end that enters the channel, while for a 3-pentoxide it is a propyl group (we refer to **Figure 4** for the visualization) encountering more interaction with the wall.

Apart from the formation of 3-pentoxide, the metadynamics simulations show that the alkoxide is only modestly more stable than the π-complex, which is in line with the earlier MD simulations.

Based on the metadynamics simulations, carbenium ions were observed and in a subsequent step these were also subjected to static periodic density functional theory calculations. When starting from configurations from the metadynamics simulations we could locate these highly elusive intermediates. The shortest C-O distance of the carbenium ion after this geometry optimization corresponds to 2.7 Å for the 2-pentyl carbenium ion and 3.4 Å for the 3-pentyl carbenium ion. The latter carbenium ion is further away from the BAS and is also about 10 kJ/mol less stable than the 2-pentyl carbenium ion. Based on the complementary set of simulations performed, we can now provide a full adsorption enthalpy diagram for all adsorbed species of 1-pentene and 2-pentene both from static and molecular dynamics simulations. This is visualized in **Figure 5** with all energy levels referred to the 1-pentene in the gas phase.

3. Conclusions

A complementary set of theoretical methods was used to fully characterize the adsorption behaviour of pentene in the pores of H-ZSM-5. Four distinct states of the olefin have been investigated: i) olefin adsorbed in the pores via dispersion forces, ii) interactions of the C=C bond of pentene with the Brønsted acid sites in the pores (π-complex), iii) the transient formation of a carbenium ion and iv) the stable formation of an alkoxide. The free physisorbed pentene was not observed during a substantial time of a molecular dynamics run at 323 K, instead a stable π-complex is rapidly formed, which does not transform towards alkoxides in a regular MD run but remains stable. This observation points towards an activated process to form stable chemisorbed species. The energies of π-complexes are very sensitive to the relative distance of the pentene molecule to the BAS. Adsorption enthalpies obtained from static calculations at 0K are systematically larger than dynamically averaged values, since only the optimized structure of the π-complex at 0 K is taken into account. Thermal fluctuations on the relative distance of the complex with the BAS give a better representation of the dynamical adsorption process and give adsorption enthalpies which are on average 20-30 kJ/mol less stable compared to their static values. Static periodic calculations have the advantage that they allow to use a large variation of DFT functionals and dispersion models. Göltl et al. observed same features for the adsorption behavior of alkanes and proposed to dynamically weight statically obtained adsorption enthalpies. [34] Based on our observations this might indeed be a good practice for future adsorption studies. Overall the π-complex and alkoxides (except the 3-pentoxide) are almost equally stable. To sample also the transformation between stable π-complexes and alkoxides the metadynamics technique was used. During the transformation we observed the carbenium ion, which seems to be a highly elusive intermediate. Furthermore the transformation from a π-complex to the carbenium ion is activated with a free energy of activation in the range of 32-36 kJ/mol in the most favorable cases. Starting from geometries taken from the metadynamics simulations we also determined the enthalpies of the carbenium ion, with static density functional theory calculations. It was confirmed that carbenium ions are transient species lying higher in energy.

Overall the present data offer a new platform for understanding the adsorption steps of olefins on zeolites in a quantitative manner, which will help, in turn, to better understand the intrinsic role of the strength of the Brønsted acid sites and the role of the local environment (siting of acid sites, available pore space) for the adsorption processes in the future.

Acknowledgments

JVdM, KDW, JH, PC, MW and VVS acknowledge the Fund for Scientific Research - Flanders (FWO), the Research Board of Ghent University (BOF), BELSPO in the frame of IAP/7/05 and the fund for scientific research Flanders (FWO) for financial support. VVS and KDW acknowledge funding from the European Union's Horizon 2020 research and innovation programme (consolidator ERC grant agreement No 647755 – DYNPOR (2015-2020)). The computational resources and services used in this work were provided by VSC (Flemish Supercomputer Center), funded by the Hercules foundation and the Flemish Government – department EWI. We would like to thank Prof. Johannes Lercher and Dr. Maricruz Sanchez-Sanchez (Department of Chemistry and Catalysis Research Center, Technische Universität München) for fruitful discussions.

References

[1] M. Guisnet, G. J.-P., Zeolites for Cleaner Technologies, Imperial College Press, London, 2002.
[2] A. Corma, Inorganic solid acids and their use in acid-catalyzed hydrocarbon reactions, Chemical reviews, 95 (1995) 559-614.
[3] J.S. Buchanan, J.G. Santiesteban, W.O. Haag, Mechanistic considerations in Acid-Catalyzed Cracking of Olefins, Journal of Catalysis, 158 (1996) 279-287.
[4] N. Rahimi, R. Karimzadeh, Catalytic cracking of hydrocarbons over modified ZSM-5 zeolites to produce light olefins: A review, Appl. Cat., A, 398 (2011) 1-17.
[5] P.A. Jacobs, J.A. Martens, In Introduction to Zeolite Science and Practice, Elsevier, Amsterdam, 1991.
[6] W. Vermeiren, J.P. Gilson, Impact of Zeolites on the Petroleum and Petrochemical Industry, Topics in Catalysis, 52 (2009) 1131-1161.
[7] Y.V. Kissin, Chemical mechanisms of catalytic cracking over solid acidic catalysts: Alkanes and alkenes, Catalysis Reviews-Science and Engineering, 43 (2001) 85-146.
[8] B.A. De Moor, M.F. Reyniers, O.C. Gobin, J.A. Lercher, G.B. Marin, Adsorption of C2-C8 n-Alkanes in Zeolites, J. Phys. Chem. C, 115 (2011) 1204-1219.
[9] F. Eder, J.A. Lercher, Alkane sorption in molecular sieves: The contribution of ordering, intermolecular interactions, and sorption on Brønsted acid sites, Zeolites, 18 (1997) 75-81.
[10] F. Eder, M. Stockenhuber, J.A. Lercher, Brønsted Acid Site and Pore Controlled Siting of Alkane Sorption in Acidic Molecular Sieves, The Journal of Physical Chemistry B, 101 (1997) 5414-5419.
[11] A. Bhan, Y.V. Joshi, W.N. Delgass, K.T. Thomson, DFT investigation of alkoxide formation from olefins in H-ZSM-5, Journal of Physical Chemistry B, 107 (2003) 10476-10487.
[12] H. Ishikawa, E. Yoda, J.N. Kondo, F. Wakabayashi, K. Domen, Stable dimerized alkoxy species of 2-methylpropene on mordenite zeolite studied by FT-IR, Journal of Physical Chemistry B, 103 (1999) 5681-5686.
[13] J.N. Kondo, S. Liqun, F. Wakabayashi, K. Domen, IR study of adsorption and reaction of 1-butene on H-ZSM-5, Catal. Lett., 47 (1997) 129-133.

[14] C.M. Nguyen, B.A. De Moor, M.-F. Reyniers, G.B. Marin, Physisorption and Chemisorption of Linear Alkenes in Zeolites: A Combined QM-Pot(MP2//B3LYP:GULP)-Statistical Thermodynamics Study, J. Phys. Chem. C, 115 (2011) 23831-23847.
[15] M. Boronat, P.M. Viruela, A. Corma, Reaction Intermediates in Acid Catalysis by Zeolites: Prediction of the Relative Tendency To Form Alkoxides or Carbocations as a Function of Hydrocarbon Nature and Active Site Structure, Journal of the American Chemical Society, 126 (2004) 3300-3309.
[16] V. Nieminen, M. Sierka, D.Y. Murzin, J. Sauer, Stabilities of C3–C5 alkoxide species inside H-FER zeolite: a hybrid QM/MM study, Journal of Catalysis, 231 (2005) 393-404.
[17] J.N. Kondo, F. Wakabayashi, K. Domen, IR Study of Adsorption of Olefins on Deuterated ZSM-5, The Journal of Physical Chemistry B, 102 (1998) 2259-2262.
[18] J.N. Kondo, K. Domen, F. Wakabayashi, Double bond migration of 1-butene without protonated intermediate on D-ZSM-5, Microporous Mesoporous Mat., 21 (1998) 429-437.
[19] E. Yoda, J.N. Kondo, K. Domen, Detailed Process of Adsorption of Alkanes and Alkenes on Zeolites, The Journal of Physical Chemistry B, 109 (2005) 1464-1472.
[20] J.N. Kondo, L. Shao, F. Wakabayashi, K. Domen, DoubleBond Migration of an Olefin without Protonated Species on H(D) Form Zeolites, The Journal of Physical Chemistry B, 101 (1997) 9314-9320.
[21] A.G. Stepanov, S.S. Arzumanov, M.V. Luzgin, H. Ernst, D. Freude, In situ monitoring of n-butene conversion on H-ferrierite by 1H, 2H, and 13C MAS NMR: kinetics of a double-bond-shift reaction, hydrogen exchange, and the 13C-label scrambling, Journal of Catalysis, 229 (2005) 243-251.
[22] M. Boronat, P. Viruela, A. Corma, Theoretical Study of the Mechanism of Zeolite-Catalyzed Isomerization Reactions of Linear Butenes, The Journal of Physical Chemistry A, 102 (1998) 982-989.
[23] A.G. Stepanov, M.V. Luzgin, S.S. Arzumanov, H. Ernst, D. Freude, n-Butene Conversion on H-Ferrierite Studied by 13C MAS NMR, Journal of Catalysis, 211 (2002) 165-172.
[24] V. Van Speybroeck, K. De Wispelaere, J. Van der Mynsbrugge, M. Vandichel, K. Hemelsoet, M. Waroquier, First principle chemical kinetics in zeolites: the methanol-to-olefin process as a case study, Chem. Soc. Rev., 43 (2014) 7326-7357.
[25] V. Van Speybroeck, K. Hemelsoet, L. Joos, M. Waroquier, R.G. Bell, C.R.A. Catlow, Advances in theory and their application within the field of zeolite chemistry, Chem. Soc. Rev., 44 (2015) 7044-7111.
[26] C. Tuma, T. Kerber, J. Sauer, The tert-Butyl Cation in H-Zeolites: Deprotonation to Isobutene and Conversion into Surface Alkoxides, Angewandte Chemie-International Edition, 49 (2010) 4678-4680.
[27] C. Tuma, J. Sauer, Protonated isobutene in zeolites: tert-butyl cation or alkoxide?, Angewandte Chemie-International Edition, 44 (2005) 4769-4771.
[28] J.B. Nicholas, J.F. Haw, The prediction of persistent carbenium ions in zeolites, Journal of the American Chemical Society, 120 (1998) 11804-11805.
[29] H. Fang, A. Zheng, J. Xu, S. Li, Y. Chu, L. Chen, F. Deng, Theoretical Investigation of the Effects of the Zeolite Framework on the Stability of Carbenium Ions, J. Phys. Chem. C, 115 (2011) 7429-7439.
[30] H. Fang, A. Zheng, S. Li, J. Xu, L. Chen, F. Deng, New Insights into the Effects of Acid Strength on the Solid Acid-Catalyzed Reaction: Theoretical Calculation Study of Olefinic Hydrocarbon Protonation Reaction, J. Phys. Chem. C, 114 (2010) 10254-10264.
[31] W.L. Dai, C.M. Wang, X.F. Yi, A.M. Zheng, L.D. Li, G.J. Wu, N.J. Guan, Z.K. Xie, M. Dyballa, M. Hunger, Identification of tert-Butyl Cations in Zeolite H-ZSM-5: Evidence from NMR Spectroscopy and DFT Calculations, Angewandte Chemie-International Edition, 54 (2015) 8783-8786.
[32] J. Sauer, M. Sierka, Combining quantum mechanics and interatomic potential functions in ab initio studies of extended systems, Journal of Computational Chemistry, 21 (2000) 1470-1493.
[33] B.A. De Moor, M.F. Reyniers, G.B. Marin, Physisorption and chemisorption of alkanes and alkenes in H-FAU: a combined ab initio-statistical thermodynamics study, Physical Chemistry Chemical Physics, 11 (2009) 2939-2958.
[34] F. Goeltl, A. Grueneis, T. Bucko, J. Hafner, Van der Waals interactions between hydrocarbon molecules and zeolites: Periodic calculations at different levels of theory, from density functional theory to the random

phase approximation and Moller-Plesset perturbation theory, Journal of Chemical Physics, 137 (2012) 114111.
[35] F. Goeltl, J. Hafner, Modelling the adsorption of short alkanes in protonated chabazite: The impact of dispersion forces and temperature, Microporous Mesoporous Mat., 166 (2013) 176-184.
[36] J.Q. Chen, A. Bozzano, B. Glover, T. Fuglerud, S. Kvisle, Recent advancements in ethylene and propylene production using the UOP/Hydro MTO process, Catalysis Today, 106 (2005) 103-107.
[37] M.J. Tallman, C. Eng, Consider new catalytic routes for olefins production - Innovative catalyst systems enable higher propylene make from liquid feedstocks, Hydrocarbon Processing, 87 (2008) 95-+.
[38] T. von Aretin, S. Schallmoser, S. Standl, M. Tonigold, J.A. Lercher, O. Hinrichsen, Single-Event Kinetic Model for 1-Pentene Cracking on ZSM-5, Industrial & Engineering Chemistry Research, 54 (2015) 11792-11803.
[39] J. Abbot, B.W. Wojciechowski, THE MECHANISM OF CATALYTIC CRACKING OF NORMAL-ALKENES ON ZSM-5 ZEOLITE, Canadian Journal of Chemical Engineering, 63 (1985) 462-469.
[40] J.S. Buchanan, The chemistry of olefins production by ZSM-5 addition to catalytic cracking units, Catalysis Today, 55 (2000) 207-212.
[41] M.A. den Hollander, M. Wissink, M. Makkee, J.A. Moulijn, Gasoline conversion: reactivity towards cracking with equilibrated FCC and ZSM-5 catalysts, Appl. Catal. A-Gen., 223 (2002) 85-102.
[42] X.X. Zhu, S.L. Liu, Y.Q. Song, L.Y. Xu, Catalytic cracking of C4 alkenes to propene and ethene: Influences of zeolites pore structures and Si/Al-2 ratios, Appl. Catal. A-Gen., 288 (2005) 134-142.
[43] G. Kresse, J. Furthmuller, Efficient iterative schemes for ab initio total-energy calculations using a plane-wave basis set, Physical Review B, 54 (1996) 11169-11186.
[44] G. Kresse, J. Furthmüller, Efficiency of ab-initio total energy calculations for metals and semiconductors using a plane-wave basis set, Comput. Mat. Sci., 6 (1996) 15.
[45] G. Kresse, J. Hafner, ABINITIO MOLECULAR-DYNAMICS FOR LIQUID-METALS, Physical Review B, 47 (1993) 558-561.
[46] G. Kresse, J. Hafner, Ab initio molecular-dynamics simulation of the liquid-metal-amorphous-semiconductor transition in germanium, Phys. Rev. B, 49 (1994) 14251.
[47] T. Verstraelen, V. Van Speybroeck, M. Waroquier, ZEOBUILDER: A GUI toolkit for the construction of complex molecular structures on the nanoscale with building blocks, Journal of Chemical Information and Modeling, 48 (2008) 1530-1541.
[48] J. Van der Mynsbrugge, S.L.C. Moors, K. De Wispelaere, V. Van Speybroeck, Insight into the Formation and Reactivity of Framework-Bound Methoxide Species in H-ZSM-5 from Static and Dynamic Molecular Simulations, Chemcatchem, 6 (2014) 1906-1918.
[49] S. Grimme, J. Antony, S. Ehrlich, H. Krieg, A consistent and accurate ab initio parametrization of density functional dispersion correction (DFT-D) for the 94 elements H-Pu, Journal of Chemical Physics, 132 (2010) 154104.
[50] P.E. Blöchl, Projector augmented-wave method, Phys. Rev. B, 50 (1994) 17953.
[51] G. Kresse, D. Joubert, From ultrasoft pseudopotentials to the projector augmented-wave method, Physical Review B, 59 (1999) 1758-1775.
[52] S. Grimme, S. Ehrlich, L. Goerigk, Effect of the Damping Function in Dispersion Corrected Density Functional Theory, Journal of Computational Chemistry, 32 (2011) 1456-1465.
[53] M. Dion, H. Rydberg, E. Schroder, D.C. Langreth, B.I. Lundqvist, Van der Waals density functional for general geometries, Phys. Rev. Lett., 92 (2004) 246401.
[54] J. Wellendorff, K.T. Lundgaard, A. Mogelhoj, V. Petzold, D.D. Landis, J.K. Norskov, T. Bligaard, K.W. Jacobsen, Density functionals for surface science: Exchange-correlation model development with Bayesian error estimation, Physical Review B, 85 (2012) 235149.
[55] A. Ambrosetti, A.M. Reilly, R.A. DiStasio, Jr., A. Tkatchenko, Long-range correlation energy calculated from coupled atomic response functions, Journal of Chemical Physics, 140 (2014).
[56] T. Bučko, S. Lebègue, T. Gould, J. Ángyán, Many-body dispersion corrections for periodic systems: an efficient reciprocal space implementation, Journal of Physics: Condensed Matter, 28 (2016) 045201.

[57] A. Ghysels, T. Verstraelen, K. Hemelsoet, M. Waroquier, V. Van Speybroeck, TAMkin: A Versatile Package for Vibrational Analysis and Chemical Kinetics, Journal of Chemical Information and Modeling, 50 (2010) 1736-1750.
[58] J. VandeVondele, M. Krack, F. Mohamed, M. Parrinello, T. Chassaing, J. Hutter, QUICKSTEP: Fast and accurate density functional calculations using a mixed Gaussian and plane waves approach, Computer Physics Communications, 167 (2005) 103-128.
[59] G. Lippert, J. Hutter, M. Parrinello, The Gaussian and augmented-plane-wave density functional method for ab initio molecular dynamics simulations, Theoretical Chemistry Accounts, 103 (1999) 124-140.
[60] G. Lippert, J. Hutter, M. Parrinello, A hybrid Gaussian and plane wave density functional scheme, Molecular Physics, 92 (1997) 477-487.
[61] K. Yang, J.J. Zheng, Y. Zhao, D.G. Truhlar, Tests of the RPBE, revPBE, tau-HCTHhyb, omega B97X-D, and MOHLYP density functional approximations and 29 others against representative databases for diverse bond energies and barrier heights in catalysis, Journal of Chemical Physics, 132 (2010) 10.
[62] S. Goedecker, M. Teter, J. Hutter, Separable dual-space Gaussian pseudopotentials, Physical Review B, 54 (1996) 1703-1710.
[63] K. De Wispelaere, B. Ensing, A. Ghysels, E.J. Meijer, V. Van Speybroeck, Complex Reaction Environments and Competing Reaction Mechanisms in Zeolite Catalysis: Insights from Advanced Molecular Dynamics, Chem.-Eur. J., 21 (2015) 9385-9396.
[64] S.L.C. Moors, K. De Wispelaere, J. Van der Mynsbrugge, M. Waroquier, V. Van Speybroeck, Molecular Dynamics Kinetic Study on the Zeolite-Catalyzed Benzene Methylation in ZSM-5, Acs Catalysis, 3 (2013) 2556-2567.
[65] F. Goltl, J. Hafner, Alkane adsorption in Na-exchanged chabazite: The influence of dispersion forces, Journal of Chemical Physics, 134 (2011) 064102.
[66] L. Schimka, J. Harl, A. Stroppa, A. Grueneis, M. Marsman, F. Mittendorfer, G. Kresse, Accurate surface and adsorption energies from many-body perturbation theory, Nat. Mater., 9 (2010) 741-744.
[67] D. Frenkel, B. Smit, Understanding Molecular Simulation, Academic Press, Inc., 2001.
[68] A. Laio, F.L. Gervasio, Metadynamics: a method to simulate rare events and reconstruct the free energy in biophysics, chemistry and material science, Rep. Prog. Phys., 71 (2008) 126601.
[69] A. Laio, M. Parrinello, Escaping free-energy minima, Proceedings of the National Academy of Sciences of the United States of America, 99 (2002) 12562-12566.
[70] K. De Wispelaere, S. Bailleul, V. Van Speybroeck, Catal. Sci. Technol., (2016).
[71] B. Ensing, A. Laio, M. Parrinello, M.L. Klein, A recipe for the computation of the free energy barrier and the lowest free energy path of concerted reactions, Journal of Physical Chemistry B, 109 (2005) 6676-6687.
[72] F. Goeltl, P. Sautet, Modeling the adsorption of short alkanes in the zeolite SSZ-13 using "van der Waals" DFT exchange correlation functionals: Understanding the advantages and limitations of such functionals, Journal of Chemical Physics, 140 (2014) 154105.
[73] C.-C. Chiu, G.N. Vayssilov, A. Genest, A. Borgna, N. Roesch, Predicting Adsorption Enthalpies on Silicalite and HZSM-5: A Benchmark Study on DFT Strategies Addressing Dispersion Interactions, Journal of Computational Chemistry, 35 (2014) 809-819.

Supplementary Material

Click here to download Supplementary Material: Adsorption of pentene SI 29 april 2016.pdf